Gradient-Based Power Minimization in MIMO Broadcast Channels With Linear Precoding

Christoph Hellings, Michael Joham, and Wolfgang Utschick

IEEE Transactions on Signal Processing

vol. 60, no. 2, Feb. 2012

Technische Universität München
Associate Institute for Signal Processing
http://www.msv.ei.tum.de

Gradient-Based Power Minimization in MIMO Broadcast Channels With Linear Precoding

Christoph Hellings, *Student Member, IEEE*, Michael Joham, *Member, IEEE*, and Wolfgang Utschick, *Senior Member, IEEE*

***Abstract*—We study the problem of minimizing the sum transmit power in mutliple-input multiple-output (MIMO) downlink channels with linear transceivers if per-user quality of service (QoS) constraints (expressed in terms of rates) have to be fulfilled. To find a suboptimal solution of the arising non-convex optimization problem, we introduce new auxiliary variables representing the division of the per-user rate constraints into per-stream rate targets, and we optimize these variables by means of gradient-projection steps. This new method is combined with alternating updates of the transmit and receive filters. Furthermore, the proposed algorithm ensures that the mean square error (MSE) matrices of all users are diagonal, and in the course of the execution of the algorithm, it is possible that inactive streams get activated if this leads to a decreased sum transmit power. In numerical simulations, the new algorithm turns out to be superior to the various existing methods since these methods either lead to a higher sum transmit power than the proposed scheme or have a higher computational complexity or make restrictive assumptions on the system parameters.**

***Index Terms*—Broadcast channels, gradient methods, linear transceivers, multiple-input multiple-output (MIMO), quality of service.**

I. Introduction

The problem of (weighted) sum rate maximization under a sum power constraint has attained considerable interest in the recent literature on multiple-input multiple-output (MIMO) communication systems (e.g., [1]–[6]). However, the solution of the weighted sum rate maximization problem cannot guarantee that all users in the system are served with an acceptable quality of service (QoS). In this paper, we will therefore study the problem of minimizing the sum transmit power subject to QoS constraints for all users, where we express the QoS in terms of achievable per-user rates. Note that the per-user rate requirements are assumed to be rigid, i.e., there is no possibility to perform user selection or scheduling. Instead, all users with non-zero rate requirement have to be served simultaneously.

The optimal solution to this problem relies on non-linear dirty-paper coding (DPC) and on time-sharing and was derived in [7]–[9]. An earlier solution approach presented in [10] was claimed to be suboptimal by the authors of [7]. Suboptimal DPC solutions with reduced complexity were proposed in [11] and [12] based on a method called block-diagonal geometric mean decomposition and in [13] based on zero-forcing and successive allocation.

However, in practice, even approximate DPC as in [14] has prohibitive complexity for online implementation. Thus, many researchers have focused on linear transceivers, which are significantly easier to implement in a practical system even though the optimization of the transmit strategy might become more involved.

Apart from the successive scheme in [13], which was also extended to systems with linear precoding, the DPC based approaches cannot be directly applied to systems with linear transceivers due to the fundamental differences between DPC and purely linear precoding. In particular, globally optimal solutions to the power minimization problem with linear transceivers are not known due to the non-concavity of the rate equations. Suboptimal solutions to this non-convex problem were proposed in [15]–[20]. The approach from [15] and [16] is based on the assumption that time-sharing between different operation points is allowed, which is an assumption that will not be adopted in this paper. In [17], a hybrid algorithm that combines block-diagonalization [21] and interference balancing (e.g., [22]) was proposed. As it is limited to the special case that the total number of receive antennas is not larger than the number of transmit antennas, it cannot be applied in the general case with arbitrary numbers of antennas. Nevertheless, we will include a system that can be solved with this method in our numerical simulations. A suboptimal solution for the general case was proposed in [18] and [19] based on a geometric programming (GP) formulation. However, despite its promising performance, this method does not seem applicable in a practical system since repeatedly solving geometric programs leads to a high computational complexity. In [20], the per-user rate, which can be exactly related to the determinant of the mean-square error (MSE) matrix [cf. (6)] for minimum mean-square error (MMSE) equalizers, has been lower-bounded using the trace of this matrix, yielding inactive rate constraints and, therefore, a sum transmit power far from the optimal value.

To overcome the various drawbacks of these existing algorithms, we propose a new gradient-based scheme that performs close to the optimal solution without having a high computational complexity and without being restricted to the case with more transmit than receive antennas. After presenting the system model in Section II, we will derive the different parts of this algorithm in Sections III through V before the method is summarized in Section VI. In the numerical simulations presented in Section VII, the performance of the new algorithm is studied and compared to the aforementioned existing

Manuscript received March 10, 2011; revised July 23, 2011; accepted September 30, 2011. Date of publication October 24, 2011; date of current version January 13, 2012. The associate editor coordinating the review of this manuscript and approving it for publication was Prof. David Love. This work was supported by Deutsche Forschungsgemeinschaft (DFG) under Grant Jo 724/1-1.

The authors are with the Associate Institute for Signal Processing, Technische Universität München, 80290 München, Germany (e-mail: hellings@tum.de; joham@tum.de; utschick@tum.de.)

Digital Object Identifier 10.1109/TSP.2011.2173337

approaches, and in Section VIII, we discuss the computational complexity of the considered algorithms.

In [2] and [23], algorithms to optimize the sum transmit power in MIMO broadcast channels under per-stream QoS constraints have been considered. However, these approaches are not applicable to the problem considered in this work as there is no explicit relation between per-stream QoS measures and per-user rates if multiple data streams per user are allowed. The same is true for the power minimization with per-user MMSE requirements proposed in [24].

A problem related to the power minimization problem is the rate balancing problem [25], which aims at maximizing the sum throughput subject to a sum power constraint and to the constraint that the rates of the individual users need to have certain fixed ratios, which are specified by a set of relative rate requirements. This problem was studied for MIMO broadcast channels with DPC in [26] and for systems with linear transceivers in [18] and [19]. In our companion work [27], we show how the algorithm presented in this paper can be adapted such that it can be applied to the rate balancing problem.

Another closely related problem is the weighted sum rate maximization under a sum power constraint and per-user rate constraints. Next to the globally optimal solutions based on DPC [28] and DPC-based heuristic solutions [29]–[31], this problem has been studied in [13], [19], and [32] for linear transceivers. In principle, the suboptimal approach from [32], which is based on a framework called signomial programming [33], can be extended to the power minimization problem. However, the exponential computational complexity of the monomial approximation from [33], which is used to solve the arising signomial programs, makes this approach unsuitable for practical implementation.

Notation: In this work, vectors are typeset in boldface lowercase letters and matrices in boldface uppercase letters. We write $\mathbf{0}$ for the zero matrix or vector and $\mathbf{I}_\bullet$ for the identity matrix of size $\bullet$. The vector $\mathbf{1}$ is the all-ones vector, and the vector $\boldsymbol{e}_i$ is the ith canonical unit vector, which has a one as the ith entry and zeros elsewhere. $[\boldsymbol{A}]_{i,j}$ is used to denote the element in the ith row and jth column of the matrix $\boldsymbol{A}$. We use $\bullet^{\mathrm{T}}$ to denote the transpose of a vector or matrix and $\bullet^{\mathrm{H}}$ for the conjugate transpose. The notation $|\bullet|$ is used for the cardinality of a set, and $\|\bullet\|_2$ for the Euclidean norm of a vector. Furthermore, $\delta_{i,j}$ is the Kronecker delta, which is 1 whenever $i=j$ and 0 otherwise. The order relation $\boldsymbol{x} \geq \boldsymbol{y}$ has to be understood element-wise, and $\mathbb{R}^n_{0,+}$ is the closed positive orthant of the $\mathbb{R}^n$, i.e., $\mathbb{R}^n_{0,+} = \{\boldsymbol{x} \in \mathbb{R}^n : \boldsymbol{x} \geq \mathbf{0}\}$. We use the shorthand notation $(\bullet_k)_{\forall k}$ for $(\bullet_1, \ldots, \bullet_K)$. For notational brevity in expressions involving variables with a superscript index and an exponent, we write $\bullet^{(i),a}$ for $(\bullet^{(i)})^a$. The same notation is used with operators that are written like an exponent, e.g., $\bullet^{(i),\mathrm{H}}$ for $(\bullet^{(i)})^{\mathrm{H}}$.

II. System Model and Problem Formulation

We consider a K-user downlink system, where the base station is equipped with M antennas while the kth receiver is equipped with N_k antennas. The frequency flat channel between the base station and user k is denoted by $\check{\boldsymbol{H}}_k^{\mathrm{H}} \in \mathbb{C}^{N_k \times M}$, and these channels are assumed to be known. The data transmission in this setting can be described by

$$\boldsymbol{y}_k = \sum_{k'=1}^{K} \check{\boldsymbol{H}}_k^{\mathrm{H}} \boldsymbol{s}_{k'} + \check{\boldsymbol{\eta}}_k \tag{1}$$

where $\check{\boldsymbol{\eta}}_k \in \mathbb{C}^{N_k}$ is additive circularly symmetric complex Gaussian noise, i.e., $\check{\boldsymbol{\eta}}_k \sim \mathcal{CN}(\mathbf{0}, \boldsymbol{C}_{\check{\boldsymbol{\eta}}_k})$, which is assumed to be independent across users and independent of the transmitted data symbols. We aim at minimizing the sum transmit power

$$P = \sum_{k=1}^{K} \mathrm{tr}[\boldsymbol{C}_{\boldsymbol{s}_k}] \tag{2}$$

where $\boldsymbol{C}_{\boldsymbol{s}_k}$ is the covariance matrix of the transmit signal $\boldsymbol{s}_k$ of user k, i.e., $\boldsymbol{s}_k \sim \mathcal{CN}(\mathbf{0}, \boldsymbol{C}_{\boldsymbol{s}_k})$, while ensuring that the rates

$$r_k = \log\det\left(\mathbf{I}_M + \boldsymbol{C}_{\boldsymbol{s}_k} \check{\boldsymbol{H}}_k \boldsymbol{C}_k^{-1} \check{\boldsymbol{H}}_k^{\mathrm{H}}\right) \tag{3}$$

with $\boldsymbol{C}_k = \boldsymbol{C}_{\check{\boldsymbol{\eta}}_k} + \sum_{k' \neq k} \check{\boldsymbol{H}}_k^{\mathrm{H}} \boldsymbol{C}_{\boldsymbol{s}_{k'}} \check{\boldsymbol{H}}_k$ fulfill the quality of service requirements $r_k \geq \varrho_k \; \forall k$. Here, ϱ_k is a given nonzero minimum rate requirement for user k. Written in terms of a mathematical optimization problem, we have to solve[1]

$$\min_{\boldsymbol{C}_{\boldsymbol{s}_1}, \ldots, \boldsymbol{C}_{\boldsymbol{s}_K}} \; P \quad \text{s.t. } r_k \geq \varrho_k \; \forall k. \tag{4}$$

Note that this optimization problem does not always have a solution. In particular, infeasibility might occur if the number of users K is larger than the number of base station antennas M and the rate requirements of the users are too demanding [34]. Therefore, a feasibility test, e.g., by means of the method proposed in [34], should be performed before the optimization procedure is started. In the remainder of this paper, we will assume that the rate requirements ϱ_k are chosen such that the problem is feasible.

A. Downlink Model With Transmit and Receive Filters

To create a transmit signal $\boldsymbol{s}_k$ with a covariance matrix $\boldsymbol{C}_{\boldsymbol{s}_k}$ whose rank is at most S_k, we can apply a beamforming matrix $\check{\boldsymbol{B}}_k = [\check{\boldsymbol{b}}_k^{(1)}, \ldots, \check{\boldsymbol{b}}_k^{(S_k)}] \in \mathbb{C}^{M \times S_k}$ to a vector of i.i.d. Gaussian unit-power data symbols $\boldsymbol{x}_k \in \mathbb{C}^{S_k}$ with $\boldsymbol{x}_k \sim \mathcal{CN}(\mathbf{0}, \mathbf{I}_{S_k})$. The beamforming matrix has to fulfill the equation $\check{\boldsymbol{B}}_k \check{\boldsymbol{B}}_k^{\mathrm{H}} = \boldsymbol{C}_{\boldsymbol{s}_k}$, i.e., for any given covariance matrix $\boldsymbol{C}_{\boldsymbol{s}_k}$, we can find infinitely many beamforming matrices $\check{\boldsymbol{B}}_k$ that only differ in a unitary rotation from the right. With $S_k = \min\{M, N_k\}$, problem (4) is equivalent to

$$\min_{\check{\boldsymbol{B}}_1, \ldots, \check{\boldsymbol{B}}_K} \sum_{k=1}^{K} \mathrm{tr}[\check{\boldsymbol{B}}_k \check{\boldsymbol{B}}_k^{\mathrm{H}}]$$
$$\text{s.t. } \log\det\left(\mathbf{I}_M + \check{\boldsymbol{B}}_k \check{\boldsymbol{B}}_k^{\mathrm{H}} \check{\boldsymbol{H}}_k \boldsymbol{C}_k^{-1} \check{\boldsymbol{H}}_k^{\mathrm{H}}\right) \geq \varrho_k \; \forall k \tag{5}$$

where $\boldsymbol{C}_k = \boldsymbol{C}_{\check{\boldsymbol{\eta}}_k} + \sum_{k' \neq k} \check{\boldsymbol{H}}_k^{\mathrm{H}} \check{\boldsymbol{B}}_{k'} \check{\boldsymbol{B}}_{k'}^{\mathrm{H}} \check{\boldsymbol{H}}_k$.

The S_k components of $\boldsymbol{x}_k$ can be interpreted as independent data streams that are to be transmitted to user k. If these streams are encoded and decoded separately, the achieved rate r_k of user k is the sum of the per-stream rates $r_k^{(s)}$, i.e., $r_k = \sum_{s=1}^{S_k} r_k^{(s)}$. Such a separate coding can be assumed without any loss in performance as long as MMSE equalization is employed and we ensure that the MSE matrix

$$\boldsymbol{E}_k^{\mathrm{DL}} = \mathrm{E}\left[(\boldsymbol{x}_k - \hat{\boldsymbol{x}}_k)(\boldsymbol{x}_k - \hat{\boldsymbol{x}}_k)^{\mathrm{H}}\right] \tag{6}$$

[1]Note that P and $r_1, \ldots, r_K$ are functions of $\boldsymbol{C}_{\boldsymbol{s}_1}, \ldots, \boldsymbol{C}_{\boldsymbol{s}_K}$; cf. (2) and (3).

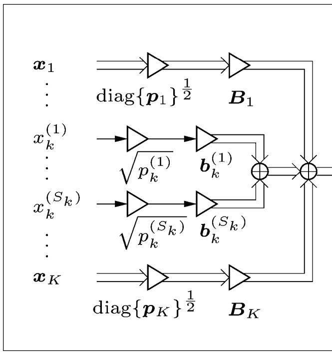

Fig. 1. Downlink system model with decomposition of user k into S_k data streams.

of each user k is diagonal [35]. In (6), $\hat{\boldsymbol{x}}_k \in \mathbb{C}^{S_k}$ is the vector of estimates given by

$$\hat{\boldsymbol{x}}_k = \check{\boldsymbol{V}}_k^{\mathrm{H}} \check{\boldsymbol{H}}_k^{\mathrm{H}} \sum_{k'=1}^{K} \check{\boldsymbol{B}}_{k'} \boldsymbol{x}_{k'} + \check{\boldsymbol{V}}_k^{\mathrm{H}} \check{\boldsymbol{\eta}}_k \tag{7}$$

where we have applied receive filters $\check{\boldsymbol{V}}_k^{\mathrm{H}} \in \mathbb{C}^{S_k \times N_k}$. Without loss of generality, we can choose the receive filters to be $\check{\boldsymbol{V}}_k^{\mathrm{H}} = \boldsymbol{V}_k^{\mathrm{H}} \boldsymbol{C}_{\check{\boldsymbol{\eta}}_k}^{-\frac{1}{2}}$, where $\boldsymbol{C}_{\check{\boldsymbol{\eta}}_k}^{\frac{1}{2}}$ is a square matrix that fulfills $\boldsymbol{C}_{\check{\boldsymbol{\eta}}_k}^{\frac{1}{2}} (\boldsymbol{C}_{\check{\boldsymbol{\eta}}_k}^{\frac{1}{2}})^{\mathrm{H}} = \boldsymbol{C}_{\check{\boldsymbol{\eta}}_k}$. This yields a system

$$\hat{\boldsymbol{x}}_k = \boldsymbol{V}_k^{\mathrm{H}} \boldsymbol{H}_k^{\mathrm{H}} \sum_{k'=1}^{K} \check{\boldsymbol{B}}_{k'} \boldsymbol{x}_{k'} + \boldsymbol{V}_k^{\mathrm{H}} \boldsymbol{\eta}_k, \tag{8}$$

with decorrelated noise $\boldsymbol{\eta}_k \sim \mathcal{CN}(\mathbf{0}, \mathbf{I}_{N_k})$, where we have considered the matrices $\boldsymbol{C}_{\check{\boldsymbol{\eta}}_k}^{-\frac{1}{2}}$ as parts of the channels $\boldsymbol{H}_k^{\mathrm{H}} = \boldsymbol{C}_{\check{\boldsymbol{\eta}}_k}^{-\frac{1}{2}} \check{\boldsymbol{H}}_k^{\mathrm{H}}$ of the whitened system. We define the matrix $\boldsymbol{B}_k = [\boldsymbol{b}_k^{(1)}, \ldots, \boldsymbol{b}_k^{(S_k)}]$ of normalized beamformers $\boldsymbol{b}_k^{(s)}$ with $\|\boldsymbol{b}_k^{(s)}\|_2 = 1$, and we introduce the downlink powers $p_k^{(s)}$ such that $\check{\boldsymbol{b}}_k^{(s)} = \sqrt{p_k^{(s)}} \boldsymbol{b}_k^{(s)}$. Then, the achievable rate of the sth stream of user k is given by

$$r_k^{(s)} = \log_2\left(1 + \gamma_k^{(s)}\right) \quad \text{with}$$

$$\gamma_k^{(s)} = \frac{p_k^{(s)} \left| \boldsymbol{v}_k^{(s),\mathrm{H}} \boldsymbol{H}_k^{\mathrm{H}} \boldsymbol{b}_k^{(s)} \right|^2}{\boldsymbol{v}_k^{(s),\mathrm{H}} \boldsymbol{v}_k^{(s)} + \sum_{\substack{k'=1 \\ (k',s') \neq (k,s)}}^{K} \sum_{s'=1}^{S_{k'}} p_{k'}^{(s')} \left| \boldsymbol{v}_k^{(s),\mathrm{H}} \boldsymbol{H}_k^{\mathrm{H}} \boldsymbol{b}_{k'}^{(s')} \right|^2} \tag{9}$$

where $\boldsymbol{v}_k^{(s),\mathrm{H}}$ is the sth row of $\boldsymbol{V}_k^{\mathrm{H}}$.

The data transmission in the whitened system is visualized in Fig. 1 both for a stream-wise and a user-wise perspective. The notation used at the receiver side for the stream-wise perspective will be introduced in Section III.

B. Optimization Problem

Just like the rates $r_k = \sum_{s=1}^{S_k} r_k^{(s)}$, we can also partition the rate requirements ϱ_k into per-stream rate targets $\rho_k^{(s)}$ that fulfill $\varrho_k = \sum_{s=1}^{S_k} \rho_k^{(s)}$. Eventually, this leads to the following reformulation of (4)[2]:

$$\min_{(\boldsymbol{B}_k, \boldsymbol{V}_k, \boldsymbol{\rho}_k, \boldsymbol{p}_k)_{\forall k}} \sum_{k=1}^{K} \sum_{s=1}^{S_k} p_k^{(s)}$$

$$\begin{aligned} \text{s.t. } & r_k^{(s)} \geq \rho_k^{(s)} \; \forall k, \; \forall s \text{ and } \sum_{s=1}^{S_k} \rho_k^{(s)} = \varrho_k \; \forall k \\ & \text{and } \rho_k^{(s)} \geq 0 \; \forall k, \; \forall s \text{ and } p_k^{(s)} \geq 0 \; \forall k, \; \forall s \\ & \text{and } \|\boldsymbol{b}_k^{(s)}\|_2 = 1 \; \forall k, \; \forall s \end{aligned} \tag{10}$$

where we have grouped the powers $p_k^{(s)}$ into vectors $\boldsymbol{p}_k = [p_k^{(1)}, \ldots, p_k^{(S_k)}]^{\mathrm{T}}$, and the rate targets $\rho_k^{(s)}$ into vectors $\boldsymbol{\rho}_k = [\rho_k^{(1)}, \ldots, \rho_k^{(S_k)}]^{\mathrm{T}}$. Apart from finding optimal filters, the main challenge is now to find the optimal rate-targets, i.e., the optimal distribution of the per-user rate requirements among the multiple data streams of each user. This difficulty has already been mentioned in [17], but no satisfying solution was given. Instead, the authors used the per-stream rates that are obtained by solving the power minimization problem with block diagonalization [21] as per-stream rate targets and kept these targets fixed throughout the execution of their algorithm. In this paper, the problem of optimizing the per-stream rate targets will be tackled by a gradient-projection approach.

To propose an algorithmic solution, we will discuss the following steps.

i) Computation of the optimal transmit power for given receive filters $(\boldsymbol{V}_k)_{\forall k}$ and per-stream rate targets $(\boldsymbol{\rho}_k)_{\forall k}$ (cf. Section III). This problem can be solved in a globally optimal manner and will be used as an inner optimization within the other steps.

ii) Gradient-projection update of the per-stream rate targets $(\boldsymbol{\rho}_k)_{\forall k}$ for given receive filters $(\boldsymbol{V}_k)_{\forall k}$ (cf. Section IV).

iii) Update of the filters. This update consists of several substeps, which will be explained in Section V.

The steps ii) and iii) are repeated in an alternating manner while i) is solved as a subproblem at certain points within the other steps.

C. Dual Uplink Model

The steps i) and ii) as well as parts of step iii) will be performed in the dual uplink, where the uplink channel matrices are given by $\boldsymbol{H}_k \in \mathbb{C}^{M \times N_k}$ and the noise is $\boldsymbol{\eta} \sim \mathcal{CN}(\mathbf{0}, \mathbf{I}_M)$:

$$\hat{\boldsymbol{\xi}}_k = \boldsymbol{U}_k^{\mathrm{H}} \sum_{k'=1}^{K} \boldsymbol{H}_{k'} \boldsymbol{T}_{k'} \boldsymbol{\xi}_{k'} + \boldsymbol{U}_k^{\mathrm{H}} \boldsymbol{\eta}. \tag{11}$$

The dual uplink is depicted in Fig. 2. The visualization also includes a stream-wise perspective, which will be introduced in Section III.

Choosing the columns $\boldsymbol{t}_k^{(s)}$ of $\boldsymbol{T}_k \in \mathbb{C}^{N_k \times S_k}$ to be the respective scaled columns of $\boldsymbol{V}_k$ and the uplink receive filters $\boldsymbol{U}_k^{\mathrm{H}} \in \mathbb{C}^{S_k \times M}$ such that their rows are the scaled rows of $\boldsymbol{B}_k^{\mathrm{H}}$, the same per-user rates can be achieved in the uplink and in the downlink with the same sum transmit power if the downlink MSE matrices (6) or the uplink MSE matrices

$$\boldsymbol{E}_k = \mathrm{E}\left[\left(\boldsymbol{\xi}_k - \hat{\boldsymbol{\xi}}_k\right)\left(\boldsymbol{\xi}_k - \hat{\boldsymbol{\xi}}_k\right)^{\mathrm{H}}\right] \tag{12}$$

are diagonal [35].

As an update of equalizers can be performed more easily than an update of beamformers, we compute the receive filter matrices $\boldsymbol{V}_k$ in the downlink (cf. Section V), but the beamforming matrices $\boldsymbol{B}_k$ are found by computing the equalizers $\boldsymbol{U}_k^{\mathrm{H}}$ in the uplink (cf. Section V).

[2]Note that each rate $r_k^{(s)}$ is a function of $(\boldsymbol{B}_k, \boldsymbol{V}_k, \boldsymbol{p}_k)_{\forall k}$; cf. (9).

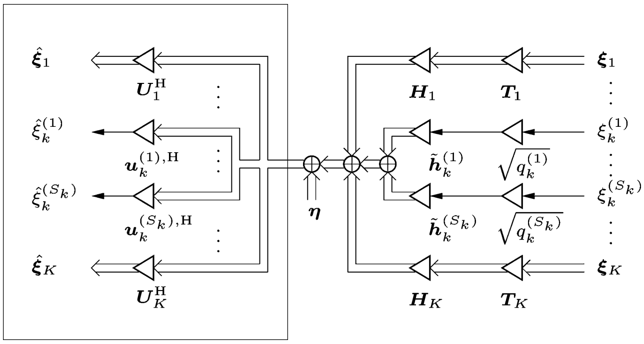

Fig. 2. Uplink system model with decomposition of user k into S_k data streams.

While most steps of the algorithm are performed stream-wise, a user-wise perspective will be taken for the uplink-to-downlink transformation, which is performed as a part of the filter update. Resorting to a user-wise perspective once per iteration suffices for the result to be meaningful for the original user-wise problem (4).

III. Optimal Sum Power for Given Filters and Per-Stream Rate Targets

In this section, we will compute the optimal sum power for given values of $(\boldsymbol{V}_k)_{\forall k}$ and $(\boldsymbol{\rho}_k)_{\forall k}$. One way to obtain this sum power is to solve the subproblem[3]

$$\begin{aligned}&\min_{(\boldsymbol{B}_k,\boldsymbol{p}_k)_{\forall k}} \sum_{k=1}^{K}\sum_{s=1}^{S_k} p_k^{(s)}\\ &\text{s.t. } r_k^{(s)} \geq \rho_k^{(s)}\ \forall k,\ \forall s \text{ and } p_k^{(s)} \geq 0\ \forall k,\ \forall s\\ &\text{and } \|\boldsymbol{b}_k^{(s)}\|_2 = 1\ \forall k,\ \forall s.\end{aligned} \tag{13}$$

Since the downlink equalizers $(\boldsymbol{V}_k)_{\forall k}$ are assumed to be fixed in this section, we can define the effective downlink channel

$$\tilde{\boldsymbol{h}}_k^{(s),\mathrm{H}} = \frac{\boldsymbol{v}_k^{(s),\mathrm{H}}}{\|\boldsymbol{v}_k^{(s)}\|_2}\boldsymbol{H}_k^{\mathrm{H}} \tag{14}$$

for the sth stream of user k, so that we get an equivalent multiple-input single-output (MISO) broadcast channel with $S_{\mathrm{tot}} = \sum_{k=1}^{K} S_k$ virtual users $_k^{(s)}$, each with a corresponding rate target $\rho_k^{(s)}$. The noise for the sth stream of user k in the effective channel is $\eta_k^{(s)} \sim \mathcal{CN}(0,1)$. The decomposition of a user k into S_k effective single-antenna users can also be seen in Fig. 1.

In this equivalent setting, problem (13) is the well-investigated problem of power minimization under per-user rate constraints in a vector broadcast channel. After testing the feasibility of the problem using the method of [34] and [36], the globally optimal solution can be found by the algorithm from [22], which is an iterative approach based on a coupling matrix describing the crosstalk between users, or by the fixed point iteration proposed in [20].

Both methods make use of a dual uplink formulation (cf. [37] and Fig. 2) with the uplink channel vectors $\tilde{\boldsymbol{h}}_k^{(s)}$ and an uplink noise covariance matrix equal to the identity matrix $\mathbf{I}_M$. In the dual uplink, the rates can be expressed in a way that they only depend on the uplink channels and the transmit powers $q_k^{(s)}$ of the SIMO uplink:

$$R_k^{(s)} = \log_2\left(1 + q_k^{(s)}\tilde{\boldsymbol{h}}_k^{(s),\mathrm{H}}\boldsymbol{X}_k^{(s),-1}\tilde{\boldsymbol{h}}_k^{(s)}\right) \tag{15}$$

with

$$\boldsymbol{X}_k^{(s)} = \mathbf{I}_M + \sum_{\substack{k'=1\\(k',s')\neq(k,s)}}^{K}\sum_{s'=1}^{S_{k'}} q_{k'}^{(s')}\tilde{\boldsymbol{h}}_{k'}^{(s')}\tilde{\boldsymbol{h}}_{k'}^{(s'),\mathrm{H}}. \tag{16}$$

From [37], it is known that a set of rates $r_k^{(s)}$ can be achieved in the downlink with a certain sum power $\sum_{k=1}^{K}\sum_{s=1}^{S_k} p_k^{(s)}$ if and only if the rates $R_k^{(s)} = r_k^{(s)}$ can be achieved in the dual uplink with appropriately chosen uplink powers fulfilling

$$\sum_{k=1}^{K}\sum_{s=1}^{S_k} q_k^{(s)} = \sum_{k=1}^{K}\sum_{s=1}^{S_k} p_k^{(s)}. \tag{17}$$

Consequently, the optimization (13) can also be performed using the uplink powers as optimization variables[4]:

$$\begin{aligned}&\min_{(\boldsymbol{q}_k)_{\forall k}} \sum_{k=1}^{K}\sum_{s=1}^{S_k} q_k^{(s)}\\ &\text{s.t. } R_k^{(s)} \geq \rho_k^{(s)}\ \forall k,\ \forall s \text{ and } q_k^{(s)} \geq 0\ \forall k,\ \forall s\end{aligned} \tag{18}$$

where $\boldsymbol{q}_k = [q_k^{(1)},\ldots,q_k^{(S_k)}]^{\mathrm{T}}$. The power $q_k^{(s)}$ can be considered as the scalar precoder of the stream $_k^{(s)}$ in the effective SIMO uplink. The corresponding precoding matrices in the dual uplink of the original MIMO system are related to these powers by [cf. Equation (14)][5]

$$\tilde{\boldsymbol{T}}_k = \left[\frac{\boldsymbol{v}_k^{(1)}}{\|\boldsymbol{v}_k^{(1)}\|_2},\ldots,\frac{\boldsymbol{v}_k^{(S_k)}}{\|\boldsymbol{v}_k^{(S_k)}\|_2}\right]\mathrm{diag}\left\{\boldsymbol{q}_k\right\}^{\frac{1}{2}}. \tag{19}$$

Having solved problem (18), the solution to (13) can be obtained by computing the optimal uplink equalizers and performing an uplink-to-downlink transformation. However, in this section, we are only interested in finding the minimal sum power for fixed $(\boldsymbol{V}_k)_{\forall k}$ and $(\boldsymbol{\rho}_k)_{\forall k}$. Thus, there is no need to immediately perform the transformation. Instead, due to (17), knowing the uplink powers $(\boldsymbol{q}_k)_{\forall k}$ suffices to also know the sum power in the downlink without even knowing the downlink strategy. Consequently, when optimizing the rate targets and filters in the next sections, the solution of problem (18) will be used to evaluate the sum power for the updated rate targets and downlink receive filters. For later reference, we define the function $\mathcal{Q}$: $\mathbb{C}^{MS_{\mathrm{tot}}} \times \mathbb{R}_{0,+}^{S_{\mathrm{tot}}} \mapsto \mathbb{R}_{0,+}^{S_{\mathrm{tot}}}$ as

$$\begin{aligned}&\mathcal{Q}\Big(\Big(\tilde{\boldsymbol{h}}_k^{(1)},\ldots,\tilde{\boldsymbol{h}}_k^{(S_k)},\boldsymbol{\rho}_k\Big)_{\forall k}\Big)\\ &= \begin{cases}\begin{pmatrix}\mathrm{argmin}_{(\boldsymbol{q}_k)_{\forall k}}\ \sum_{k=1}^{K}\sum_{s=1}^{S_k} q_k^{(s)}\\ \text{s.t. } R_k^{(s)} \geq \rho_k^{(s)}\ \forall k,\ \forall s\\ \text{and } q_k^{(s)} \geq 0\ \forall k,\ \forall s\end{pmatrix} & \text{if feasible}\\ \Big([\infty,\ldots,\infty]^{\mathrm{T}}\Big)_{\forall k} & \text{otherwise}\end{cases}\end{aligned} \tag{20}$$

[3]Note that each rate $r_k^{(s)}$ is a function of the optimization variables $(\boldsymbol{B}_k,\boldsymbol{p}_k)_{\forall k}$ and of the fixed variables $(\boldsymbol{V}_k)_{\forall k}$; cf. (9).

[4]Note that for fixed effective channels $(\tilde{\boldsymbol{h}}_k^{(1)},\ldots,\tilde{\boldsymbol{h}}_k^{(S_k)})_{\forall k}$, each uplink rate $R_k^{(s)}$ is a function of the uplink powers $(\boldsymbol{q}_k)_{\forall k}$; cf. (15).

[5]In this equation, $\tilde{\boldsymbol{T}}_k$ is used for the uplink beamforming matrix (instead of $\boldsymbol{T}_k$) as we will later apply a unitary rotation to this matrix in order to obtain the eventual uplink beamforming matrix $\boldsymbol{T}_k$; see (31).

which encapsulates the implementation of the solver of problem (18).

IV. Gradient-Based Update of the Per-Stream Rate Targets

We propose to update the per-stream rate targets by a gradient step

$$\tilde{\rho}_k^{(s)} \leftarrow \rho_k^{(s)} - d \frac{\partial P}{\partial \rho_k^{(s)}} \quad \forall k, \forall s \tag{21}$$

followed by a projection to the set of valid rate targets. In the following, we will state and proof the calculation rule of the gradient as well as the projection operation. Afterwards, we will discuss the choice of the step size d.

To calculate the gradient of the sum transmit power with respect to the per-stream rate targets $\rho_k^{(s)}$, we choose a dual uplink formulation as in Section III, i.e., we express the sum power by $P = \sum_{k'=1}^{K} \sum_{s'=1}^{S_{k'}} q_{k'}^{(s')}$ and calculate its partial derivatives with respect to the rate targets. To do so, the following proposition is helpful.

Proposition 1: The Jacobian matrix $\boldsymbol{J}_R \in \mathbb{R}^{S_{\text{tot}} \times S_{\text{tot}}}$ of the rates $R_\kappa^{(\sigma)}$ with respect to the uplink powers $q_{k'}^{(s')}$, defined as

$$[\boldsymbol{J}_R]_{\sigma + \sum_{j=1}^{\kappa-1} S_j,\, s' + \sum_{j=1}^{k'-1} S_j} = \frac{\partial R_\kappa^{(\sigma)}}{\partial q_{k'}^{(s')}}, \tag{22}$$

is inverse-positive, i.e., $\boldsymbol{J}_R^{-1}$ exists and has only non-negative entries.

Proof: See Appendix A. ■

Now, we can formulate the main Theorem of this section, which states the calculation rule of the gradient.

Theorem 1: The partial derivatives of the sum power $P = \sum_{k'=1}^{K} \sum_{s'=1}^{S_{k'}} q_{k'}^{(s')}$ with respect to the rate targets $\rho_k^{(s)}$ are given by

$$\frac{\partial P}{\partial \rho_k^{(s)}} = \mathbf{1}^{\mathrm{T}} \boldsymbol{J}_R^{-1} \boldsymbol{e}_k^{(s)} \geq 0 \tag{23}$$

where $\boldsymbol{J}_R$ is the Jacobian matrix defined in (22), and $\boldsymbol{e}_k^{(s)} = \boldsymbol{e}_{s + \sum_{j=1}^{k-1} S_j}$.

Proof: See Appendix B. ■

Since all partial derivatives $\frac{\partial P}{\partial \rho_k^{(s)}}$ are non-negative, the sum $\sum_{s=1}^{S_k} \tilde{\rho}_k^{(s)}$ of the new rate targets of user k obtained from the gradient update (21) is smaller than the per-user rate requirement ϱ_k in general, and the following projection is necessary.

Lemma 1: The projection of the per-stream rate targets $\tilde{\rho}_k^{(1)}, \ldots, \tilde{\rho}_k^{(S_k)}$ to the set of per-stream rate targets feasible for user k in the sense of minimal Euclidean distance is given by the waterfilling equation

$$\rho_k^{(s)} = \max\left\{\tilde{\rho}_k^{(s)} + \mu_k,\, 0\right\} \tag{24}$$

with the water level

$$\mu_k = \frac{1}{|\mathcal{S}_{k,\mathrm{a}}|} \left(\varrho_k - \sum_{s \in \mathcal{S}_{k,\mathrm{a}}} \tilde{\rho}_k^{(s)} \right) \tag{25}$$

where $\mathcal{S}_{k,\mathrm{a}}$ is the set of active streams of user k.

Proof: See [38] or Appendix C. ■

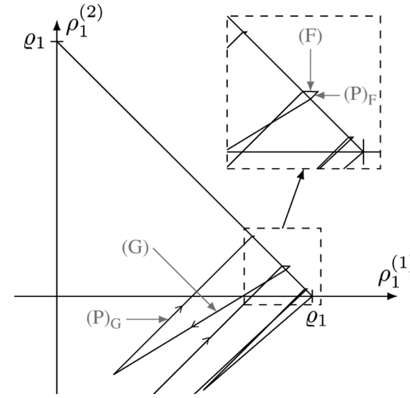

Fig. 3. Development of the per-stream rate targets of a user during three iterations: (G)radient steps, (P)rojections, and adaptations after the (F)ilter updates.

Sorting the streams with respect to $\tilde{\rho}_k^{(s)}$, the optimal water level μ_k can be found by a linear search for $|\mathcal{S}_{k,\mathrm{a}}| \in \{1, \ldots, S_k\}$.

In Fig. 3,[6] we can observe that the gradient step (G) reduces all per-stream rate targets. Therefore, a projection back to the set of valid rate targets, i.e., to the diagonal line segment representing the per-user rate requirement ϱ_k, is necessary. This corresponds to the step $(\mathrm{P})_\mathrm{G}$ that follows right after (G) in Fig. 3. After the gradient step (G) and the projection $(\mathrm{P})_\mathrm{G}$, the sum transmit power is lower than it was before these steps if the step size d is chosen properly.

A proper choice of the step size is necessary since the gradient-projection update makes a step in an improving direction, but the improvement can be guaranteed only locally. Therefore, the sum transmit power, which can be computed by means of the function $\mathcal{Q}$ defined in (20), might be increased after the gradient-projection step, which indicates that a too large step size d was used. To avoid this situation, we introduce the following step size adaptation: we start with an initial step size d_{init}, and if the gradient-projection leads to a degradation instead of an improvement,[7] we repeatedly reduce the step size by a factor of two and retry the gradient-projection step until a decrease in sum power is eventually achieved. The method is robust to the choice of the initial step size, but the execution of the algorithm can be slow if a very large or very small initial value is chosen. The choice $d_{\text{init}} = \frac{1}{2}$ worked well in our simulations. If the sum transmit power cannot be decreased even with a very small step size (smaller than a given limit $d_{\min}$, which was set to 2^{-20} in our simulations), an improvement is locally no longer possible, and a stationary point with respect to the per-stream rate targets has been reached. In this case, the old rate targets are kept, and the algorithm proceeds to the filter update without having changed the rate targets.

V. Update of the Filters

In this section, we will propose an update procedure for the transmit and receive filters. First, we will discuss four main steps of the filter update. Afterwards, we will explain how the per-stream rate targets can be adapted after the filter update in order to achieve a reduction of the sum transmit power.

[6]This figure corresponds to iteration 5 through 7 of the numerical results that will be presented later in Fig. 5

[7]Since the function $\mathcal{Q}$ maps infeasible rate targets to infinite transmit power, they are only a special case of an increased sum transmit power.

A. Update of the Uplink Receive Filters

When calculating the optimal uplink powers based on the rate expression (15) in Section III, it was implicitly assumed that the uplink receive filters are chosen such that they deliver sufficient statistics for the intended parts of the received signals. As our considerations are stream-wise, a sufficient statistic has to be delivered for each stream individually, which is fulfilled by the optimal receivers in the MMSE sense given by[8]

$$\tilde{\boldsymbol{U}}_k^{\mathrm{H}} = \mathrm{diag}\left\{\boldsymbol{q}_k\right\}^{\frac{1}{2}} \tilde{\boldsymbol{H}}_k^{\mathrm{H}} \boldsymbol{X}^{-1} \tag{26}$$

with

$$\boldsymbol{X} = \mathbf{I}_M + \sum_{k=1}^{K}\sum_{s=1}^{S_k} q_k^{(s)} \tilde{\boldsymbol{h}}_k^{(s)} \tilde{\boldsymbol{h}}_k^{(s),\mathrm{H}} \tag{27}$$

where $\boldsymbol{q}_k = [q_k^{(1)},\ldots,q_k^{(S_k)}]^{\mathrm{T}}$, $\tilde{\boldsymbol{H}}_k = \left[\tilde{\boldsymbol{h}}_k^{(1)},\ldots,\tilde{\boldsymbol{h}}_k^{(S_k)}\right]$, and $\tilde{\boldsymbol{h}}_k^{(s)}$ is given by (14). Note that the computation of $\tilde{\boldsymbol{U}}_k$ with (26) corresponds to an update of the respective downlink precoding matrix $\check{\boldsymbol{B}}_k$.

B. Diagonalization of the MSE Matrices

We will now make use of the following result from [35]:

Lemma 2: Decoding the received signal of a user in a stream-wise manner is optimal if and only if the uplink MSE matrix

$$\boldsymbol{E}_k = \mathbf{I}_{S_k} + \tilde{\boldsymbol{U}}_k^{\mathrm{H}} \boldsymbol{X} \tilde{\boldsymbol{U}}_k - \tilde{\boldsymbol{U}}_k^{\mathrm{H}} \tilde{\boldsymbol{H}}_k \mathrm{diag}\left\{\boldsymbol{q}_k\right\}^{\frac{1}{2}} - \mathrm{diag}\left\{\boldsymbol{q}_k\right\}^{\frac{1}{2}} \tilde{\boldsymbol{H}}_k^{\mathrm{H}} \tilde{\boldsymbol{U}}_k \tag{28}$$

$$= \mathbf{I}_{S_k} - \mathrm{diag}\left\{\boldsymbol{q}_k\right\}^{\frac{1}{2}} \tilde{\boldsymbol{H}}_k^{\mathrm{H}} \boldsymbol{X}^{-1} \tilde{\boldsymbol{H}}_k \mathrm{diag}\left\{\boldsymbol{q}_k\right\}^{\frac{1}{2}} \tag{29}$$

is diagonal. Moreover, if this is the case, a stream-wise uplink-to-downlink transformation preserves the per-user rates.

Sketch of Proof: For the sum rate of user k, we have

$$\sum_{s=1}^{S_k} R_k^{(s)} \leq -\log\det \boldsymbol{E}_k \tag{30}$$

where $R_k^{(s)}$ are the per-stream rates in the uplink and the right-hand side of the inequality is the per-user sum rate achievable in the uplink with joint decoding of the streams of user k [39]. Equality holds in (30) if and only if $\boldsymbol{E}_k$ is diagonal.[9] As $r_k^{(s)} = R_k^{(s)}$ holds for the per-stream rates $r_k^{(s)}$ in the downlink after a stream-wise uplink-to-downlink transformation [37], the same per-user sum rate is achievable in the downlink. The proof is completed by also showing the converse, i.e., showing that no higher rate can be achieved in the downlink with joint decoding of the streams of user k; cf. [35]. ■

To diagonalize $\boldsymbol{E}_k$, the filters of the MIMO uplink have to be chosen according to [cf. (19) and (26)]

$$\boldsymbol{T}_k = \tilde{\boldsymbol{T}}_k \boldsymbol{F}_k = \left[\frac{\boldsymbol{v}_k^{(1)}}{\|\boldsymbol{v}_k^{(1)}\|_2},\ldots,\frac{\boldsymbol{v}_k^{(S_k)}}{\|\boldsymbol{v}_k^{(S_k)}\|_2}\right] \mathrm{diag}\left\{\boldsymbol{q}_k\right\}^{\frac{1}{2}} \boldsymbol{F}_k, \tag{31}$$

$$\boldsymbol{U}_k^{\mathrm{H}} = \boldsymbol{F}_k^{\mathrm{H}} \tilde{\boldsymbol{U}}_k^{\mathrm{H}} \tag{32}$$

where $\boldsymbol{F}_k \in \mathbb{C}^{S_k \times S_k}$ is the modal matrix of the eigenvalue decomposition

$$\boldsymbol{F}_k \boldsymbol{D}_k \boldsymbol{F}_k^{\mathrm{H}} = \mathrm{diag}\left\{\boldsymbol{q}_k\right\}^{\frac{1}{2}} \tilde{\boldsymbol{H}}_k^{\mathrm{H}} \boldsymbol{X}^{-1} \tilde{\boldsymbol{H}}_k \mathrm{diag}\left\{\boldsymbol{q}_k\right\}^{\frac{1}{2}}. \tag{33}$$

When calculating the MSE matrix and the optimal filters of the other users, $\boldsymbol{F}_k$ cancels out, i.e., the diagonalization of the MSE matrix $\boldsymbol{E}_k$ of user k does not have any influence on the streams of other users. Furthermore, since $\boldsymbol{F}_k$ is a unitary matrix, the sum of the transmitted power is not changed, i.e., $\mathrm{tr}[\boldsymbol{T}_k \boldsymbol{T}_k^{\mathrm{H}}] = \mathrm{tr}[\tilde{\boldsymbol{T}}_k \tilde{\boldsymbol{T}}_k^{\mathrm{H}}]$, and the right-hand side of the inequality in (30) is invariant to the unitary rotation in (31) and (32). Thus, the diagonalization of the MSE matrix $\boldsymbol{E}_k$ increases the current per-user rate $r_k = \sum_{s=1}^{S_k} R_k^{(s)}$ of user k achievable with separate decoding.

C. Uplink-to-Downlink Transformation

After the diagonalization, the system can be transformed to a downlink system by choosing

$$\boldsymbol{b}_k^{(s)} \leftarrow \frac{\boldsymbol{u}_k^{(s)}}{\|\boldsymbol{u}_k^{(s)}\|_2} \text{ and } \boldsymbol{v}_k^{(s)} \leftarrow \boldsymbol{t}_k^{(s)} \tag{34}$$

and calculating the downlink powers $\boldsymbol{p}_k = [p_k^{(1)},\ldots,p_k^{(S_k)}]^{\mathrm{T}}$ using

$$\boldsymbol{M}\left[\boldsymbol{p}_1^{\mathrm{T}},\ldots,\boldsymbol{p}_K^{\mathrm{T}}\right]^{\mathrm{T}} = \boldsymbol{\tau} \tag{35}$$

with $[\boldsymbol{\tau}]_{s+\sum_{j=1}^{k-1} S_j} = \|\boldsymbol{t}_k^{(s)}\|_2^2$ and

$$\boldsymbol{M} = \begin{bmatrix} \boldsymbol{M}_{1,1} & \ldots & \boldsymbol{M}_{1,K} \\ \vdots & \ddots & \vdots \\ \boldsymbol{M}_{K,1} & \ldots & \boldsymbol{M}_{K,K} \end{bmatrix} \in \mathbb{R}^{S_{\mathrm{tot}} \times S_{\mathrm{tot}}} \tag{36}$$

where $[\boldsymbol{M}_{\kappa,k}]_{\sigma,s} = -|\boldsymbol{u}_k^{(s),\mathrm{H}} \boldsymbol{H}_\kappa \boldsymbol{t}_\kappa^{(\sigma)}|^2$ for $\kappa \neq k$ and $\boldsymbol{M}_{k,k} = \mathrm{diag}_{s=1}^{S_k}\left\{\|\boldsymbol{u}_k^{(s)}\|_2^2 - \sum_{\kappa\neq k} \mathbf{1}^{\mathrm{T}} \boldsymbol{M}_{\kappa,k} \boldsymbol{e}_s\right\}$ were introduced in [35].

D. Update of the Downlink Receive Filters

Note that the equalizers $\boldsymbol{v}_k^{(s)}$ resulting from the uplink-to-downlink transformation do not deliver sufficient statistics for the respective data streams. Therefore, we optimize the downlink receive filters such that they minimize the MSE by choosing

$$\boldsymbol{v}_k^{(s),\mathrm{H}} \leftarrow \sqrt{p_k^{(s)}} \boldsymbol{b}_k^{(s),\mathrm{H}} \boldsymbol{H}_k \boldsymbol{Y}_k^{-1} \tag{37}$$

for all ${}_k^{(s)}$ with $p_k^{(s)} \neq 0$, where

$$\boldsymbol{Y}_k = \mathbf{I}_{N_k} + \boldsymbol{H}_k^{\mathrm{H}} \left(\sum_{k'=1}^{K} \boldsymbol{B}_{k'} \mathrm{diag}\left\{\boldsymbol{p}_{k'}\right\} \boldsymbol{B}_{k'}^{\mathrm{H}}\right) \boldsymbol{H}_k. \tag{38}$$

The rates of the individual streams and, consequently, the sum rate of each user, is increased by this update.

Applied to inactive streams with $p_k^{(s)} = 0$, the filter update would set the filters of these streams to zero vectors so that the definition of an effective MISO channel $\tilde{\boldsymbol{h}}_k^{(s),\mathrm{H}}$ in (14) would

[8]In this equation, $\tilde{\boldsymbol{U}}_k^{\mathrm{H}}$ is used for the uplink receive filter (instead of $\boldsymbol{U}_k^{\mathrm{H}}$) as we will later apply a unitary rotation to this matrix in order to obtain the eventual uplink receive filter $\boldsymbol{U}_k^{\mathrm{H}}$, see (32).

[9]Using the fact that $\tilde{\boldsymbol{H}}_k^{\mathrm{H}} \boldsymbol{X}^{-1} \tilde{\boldsymbol{H}}_k = \mathrm{diag}\left\{\tilde{\boldsymbol{h}}_k^{(s),\mathrm{H}} \boldsymbol{X}^{-1} \tilde{\boldsymbol{h}}_k^{(s)}\right\}_{s=1}^{S_k}$ holds if $\boldsymbol{E}_k$ is diagonal, the right side of the inequality can be written as $-\log\prod_{s=1}^{S_k}(1+q_k^{(s)} \tilde{\boldsymbol{h}}_k^{(s),\mathrm{H}} \boldsymbol{X}^{-1} \tilde{\boldsymbol{h}}_k^{(s)})$, and equality can be shown by applying (15), (46), and (45) to the left side of the inequality.

be impossible for these streams. Therefore, we propose to exclude the filters of inactive streams from the update (37) and to perform the procedure described in Appendix D instead. This method is based on computing a generalized eigenvalue decomposition (GEVD) for each inactive stream.

Recall that we have diagonalized the uplink MSE matrices in (31) and (32) after the update of the uplink equalizers in (26). This was done for two reasons: optimality of stream-wise coding in the case of diagonal MSE matrices and the necessity of the diagonalization as a part of the uplink-to-downlink transformation described in [35]. In the downlink, such a diagonalization is not necessary. For the MSE matrices to be diagonal after convergence, one diagonalization per iteration is sufficient, and for the downlink-to-uplink transformation, the shape of the MSE matrices is not important since the transformation is meant to be stream-wise (cf. Section III) and not user-wise.

E. Adaptation of the Per-Stream Rate Targets

At this point, the sum transmit power still equals the value it had at the beginning of the filter update, but the per-user rates of all users are increased by the diagonalization of the MSE matrices and by the filter update in the downlink. Thus, a reduced transmit power would be sufficient to fulfill the per-user rate requirements with equality. To this end, the power allocation has to be recomputed with the function $\mathcal{Q}$ defined in (20). However, the unitary rotations needed to diagonalize the MSE matrices have destroyed the mapping between the per-stream rate targets $\rho_k^{(s)}$ and the actual data streams since the streams might have been resorted or even recombined. We therefore make a new choice for the per-stream rate targets in a way that the total power is reduced.

To this end, we simply set the per-stream rate targets $\tilde{\boldsymbol{\rho}}_k = [\tilde{\rho}_k^{(1)}, \ldots, \tilde{\rho}_k^{(S_k)}]^{\mathrm{T}}$ to the currently achieved per-stream rates $\boldsymbol{r}_k = [r_k^{(1)}, \ldots, r_k^{(S_k)}]^{\mathrm{T}}$ for all users k. The sum of these new rate targets is higher than the per-user rate constraint, as can also be observed in step (F) in Fig. 3. Recomputing the uplink powers corresponding to these per-stream rate targets $\tilde{\rho}_k^{(s)}$ by means of the function $\mathcal{Q}$, we would get the same sum transmit power as before. However, if we apply the orthogonal projection from Lemma 1, which is called $(\mathrm{P})_{\mathrm{F}}$ in Fig. 3, all per-stream rate targets are reduced since the rate target vector after step (F) lies above the line segment of feasible targets. Consequently, evaluating the function $\mathcal{Q}$ with the projected targets $\boldsymbol{\rho}_k = [\rho_k^{(1)}, \ldots, \rho_k^{(S_k)}]^{\mathrm{T}} \leq \tilde{\boldsymbol{\rho}}_k$ for all users k delivers a sum transmit power that is guaranteed to be lower than or equal to the power before the whole filter update.

VI. The Algorithm at a Glance

Having discussed all ingredients of the method, we can now summarize it in Algorithm 1. The general concept can be described as follows.

- The per-stream rate targets $\rho_k^{(s)}$, the downlink transmit filters $\check{\boldsymbol{B}}_k$, and the downlink receive filters $\boldsymbol{V}_k^{\mathrm{H}}$ are updated in an alternating manner.
- While a gradient-projection step is performed for the rate targets, the filters are computed as MMSE equalizers in the uplink and in the downlink, respectively.
- The optimization of the power allocation, which was introduced in Section III, is not a step on its own, but rather an inner optimization, which is solved at certain points within the other steps. In particular, it is used to compute the current sum power within the gradient-projection step in order to allow a step size adaptation, and it is solved after the update of the filters in order to benefit from the new filters in terms of a reduced transmit power.

Algorithm 1: Gradient-Based QoS Algorithm for MIMO BC

Require: $(\varrho_k)_{\forall k}$, $(\boldsymbol{H}_k)_{\forall k}$, $(\boldsymbol{V}_k)_{\forall k}$, $(\boldsymbol{\rho}_k)_{\forall k}$, $\epsilon, d_{\mathrm{init}}, d_{\mathrm{min}}$

(1) $(\boldsymbol{q}_k)_{\forall k} \leftarrow \mathcal{Q}\left(\left(\tilde{\boldsymbol{h}}_k^{(1)}, \ldots, \tilde{\boldsymbol{h}}_k^{(S_k)}, \boldsymbol{\rho}_k\right)_{\forall k}\right)$, $\tilde{\boldsymbol{h}}_k^{(s)}$ from (14)

(2) **repeat**

(3) $\quad \boldsymbol{q}_{k,\mathrm{last}} \leftarrow \boldsymbol{q}_k \ \forall k$

(4) $\quad$ compute the uplink receivers $\tilde{\boldsymbol{U}}_k^{\mathrm{H}}$ using (26)

(5) $\quad$ diagonalize the MSE matrices using (31) and (32)

(6) $\quad$ perform UL to DL transformation using (34) and (35)

(7) $\quad$ compute the downlink receivers $\boldsymbol{v}_k^{(s),\mathrm{H}}$ of active streams using (37)

(8) $\quad$ compute the new per-stream rates $(\boldsymbol{r}_k)_{\forall k}$ using (9)

(9) $\quad$ compute the rate targets $(\boldsymbol{\rho}_k)_{\forall k}$ by applying projection rule (24) to $(\tilde{\boldsymbol{\rho}}_k)_{\forall k} \leftarrow (\boldsymbol{r}_k)_{\forall k}$

(10) $\quad (\boldsymbol{q}_k)_{\forall k} \leftarrow \mathcal{Q}\left(\left(\tilde{\boldsymbol{h}}_k^{(1)}, \ldots, \tilde{\boldsymbol{h}}_k^{(S_k)}, \boldsymbol{\rho}_k\right)_{\forall k}\right)$, $\tilde{\boldsymbol{h}}_k^{(s)}$ from (14)

(11) $\quad$ compute the downlink receivers $\boldsymbol{v}_k^{(s),\mathrm{H}}$ of inactive streams by repeatedly solving (68)

(12) $\quad$ compute the gradient using (23)

(13) $\quad d \leftarrow d_{\mathrm{init}}$

(14) $\quad$ **loop**

(15) $\quad\quad$ compute $(\tilde{\boldsymbol{\rho}}_k)_{\forall k}$ by performing the gradient step (21) with step size d

(16) $\quad\quad$ compute the rate targets $(\boldsymbol{\rho}_{k,\mathrm{new}})_{\forall k}$ by applying projection rule (24) to $(\tilde{\boldsymbol{\rho}}_k)_{\forall k}$

(17) $\quad\quad (\boldsymbol{q}_{k,\mathrm{new}})_{\forall k} \leftarrow \mathcal{Q}\left(\left(\tilde{\boldsymbol{h}}_k^{(1)}, \ldots, \tilde{\boldsymbol{h}}_k^{(S_k)}, \boldsymbol{\rho}_{k,\mathrm{new}}\right)_{\forall k}\right)$, $\tilde{\boldsymbol{h}}_k^{(s)}$ from (14)

(18) $\quad\quad$ **if** $\sum_{k=1}^K \mathbf{1}^{\mathrm{T}} \boldsymbol{q}_{k,\mathrm{new}} \leq \sum_{k=1}^K \mathbf{1}^{\mathrm{T}} \boldsymbol{q}_k$ **then**

(19) $\quad\quad\quad \boldsymbol{\rho}_k \leftarrow \boldsymbol{\rho}_{k,\mathrm{new}}, \ \ \boldsymbol{q}_k \leftarrow \boldsymbol{q}_{k,\mathrm{new}} \ \forall k$

(20) $\quad\quad\quad$ **break**

(21) $\quad\quad$ **else if** $d < d_{\mathrm{min}}$ **then**

(22) $\quad\quad\quad$ **break**

(23) $\quad\quad$ **end if**

(24) $\quad\quad d \leftarrow \frac{d}{2}$

(25) $\quad$ **end loop**

(26) **until** $\left(\sum_{k=1}^K \mathbf{1}^{\mathrm{T}} \mathbf{q}_{k,\mathrm{last}} - \sum_{k=1}^K \mathbf{1}^{\mathrm{T}} \mathbf{q}_k\right) \leq \epsilon$

(27) transform the obtained strategy to the downlink

Convergence of the algorithm with respect to the sum transmit power P is guaranteed since neither the gradient-projection step from Section IV nor the filter update from Section V can increase the sum power and, on the other hand, the sum power is bounded from below by the optimal value. To detect convergence, the decrease in sum power between the last and the current iteration is compared to a small constant ϵ. We chose $\epsilon = 10^{-4}$ in our simulations.

The downlink receive filters $\boldsymbol{v}_k^{(s),\mathrm{H}}$ and the rate targets $\rho_k^{(s)}$ have to be initialized such that the innermost problem (18) has a feasible solution in the first iteration. In our simulations, we have used

$$\rho_k^{(s)} = \begin{cases} \varrho_k & \text{if } s = 1, \\ 0 & \text{otherwise} \end{cases} \tag{39}$$

which is a reasonable choice since any feasible rates can be achieved with single-stream transmission in a MIMO broadcast channel with linear transceivers [34]. However, the result from [34] only states that it is possible to find filters for which the per-stream rate targets (39) are feasible. Thus, the initial receive filters have to be chosen properly, too. In particular, feasibility might be impaired if the downlink receive filters are chosen such that the effective channels $\tilde{\boldsymbol{h}}_k^{(s)}$ violate the regularity condition [36]

$$\mathrm{Rank}\left[\tilde{\boldsymbol{H}}_{\mathcal{S}}\right] = \min(|\mathcal{S}|, M) \;\; \forall \mathcal{S} \subseteq \bigcup_{k=1}^{K} \left\{ {}_k^{(1)}, \ldots, {}_k^{(S_k)} \right\} \tag{40}$$

where $\tilde{\boldsymbol{H}}_{\mathcal{S}} \in \mathbb{C}^{|\mathcal{S}| \times M}$ is a matrix whose rows are the effective channel vectors $\tilde{\boldsymbol{h}}_k^{(s),\mathrm{H}}$ for all streams s of all users k with ${}_k^{(s)} \in \mathcal{S}$.[10] In the special case that the channel matrices $\boldsymbol{H}_k$ have i.i.d. Gaussian entries, the regularity condition is fulfilled almost surely if we choose (random or deterministic) initial filter vectors $\boldsymbol{v}_k^{(s)}$ such that all filters of a user are linearly independent. In this case, a possible choice, which was also used in our simulations, is

$$\boldsymbol{v}_k^{(s)} = \boldsymbol{e}_s. \tag{41}$$

VII. Discussion and Numerical Results

In this section, we will evaluate the performance of the proposed method by means of numerical simulations. As transmitting more data streams than the base station has degrees of freedom leads to an interference limited setup, three qualitatively different scenarios can be considered:

1) $M \geq \sum_{k=1}^{K} N_k$, i.e., more transmit antennas than the total number of receive antennas. If this is the case, block-diagonalization [21] can be performed, and each user can be served with up to N_k data streams. In our simulations, we will consider a system with $M = 20$ base station antennas, $K = 4$ users, and $N_k = 5$ receive antennas for each user k.
2) $M \leq K$, i.e., less transmit antennas than the number of users. To keep the number of data streams as close as possible to the number of degrees of freedom M, we expect the algorithm to converge to a solution where each user is served with only one data stream. Indeed, this is what happens in numerical simulations. However, the novel techniques used in the algorithm, i.e., the gradient-based adaptation of the per-stream rate targets and the possibility to activate inactive streams, do not have any effect in the case of a single data stream per user. Consequently, for $M \leq K$, the algorithm is nothing but an alternating optimization of the transmit and receive filters for single-stream transmission. We, therefore, do not consider this case in the simulations. Also note that in the case $M < K$, the problem might be infeasible if the rate requirements ϱ_k are too high [34].
3) $K < M < \sum_{k=1}^{K} N_k$, i.e., more transmit antennas than the number of users, but less than the total number of receive antennas. Now, more than one data stream can be used for some users, but it is not possible to serve all users with N_k streams. This scenario will be considered for a four-user system with $M = 10$ and $N_k = 5$ as well as for a three-user system with $M = 4$ and $N_k = 2$.

[10]In the case where there are already singularities in the original channel matrices, i.e., no filter vectors fulfilling the regularity condition on the effective channels exist, different choices of filters will still yield a different number of rank deficiencies and, thus, different feasibility regions.

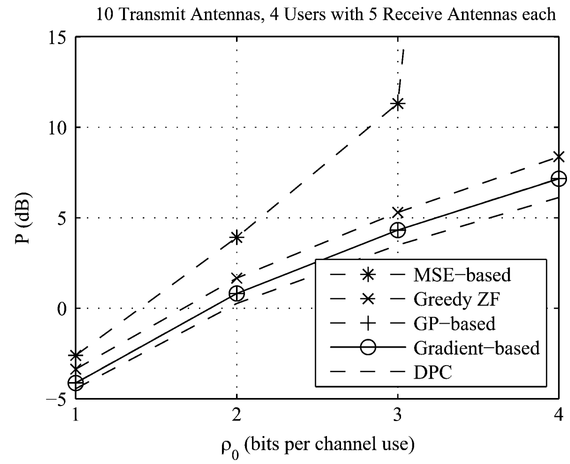

Fig. 4. Transmit power for different per-user rate requirements.

We perform the simulations with $\varrho_1 = \varrho_2 = 2\rho_0$ and $\varrho_3 = \varrho_4 = \rho_0$ for various values of ρ_0, where ϱ_4 is ignored in case of a three-user system. All channel coefficients are i.i.d. circularly symmetric complex Gaussian with zero mean and unit variance, and the noise covariance matrices are always assumed to be $\boldsymbol{C}_{\tilde{\boldsymbol{\eta}}_k} = \mathbf{I}_{N_k}$. The resulting powers are averaged over 1000 realizations of the involved random variables by means of the geometric mean, which is equivalent to taking the arithmetic mean in the dB domain.

In Fig. 4, we consider the four-user MIMO system with $M = 10$ transmit antennas and $N_k = 5$ receive antennas for each user k. For comparison, we have implemented a zero-forcing (ZF) scheme with greedy user allocation (cf. [13]), the geometric programming (GP) based method from [19], and the MSE-based QoS optimization from [20]. Out of these three schemes, the GP-based method is the only one that achieves an average sum transmit power comparable to the power achieved by the gradient-projection approach. However, as will be discussed in the next section, the computational complexity of the GP-based algorithm is significantly higher. The MSE-based scheme systematically underestimates the achieved rates, i.e., after convergence, the per-user rates are higher than requested, which is one of the reasons for the high transmit power of this scheme. Obviously, this effect is particularly strong for cases with very demanding rate requirements.

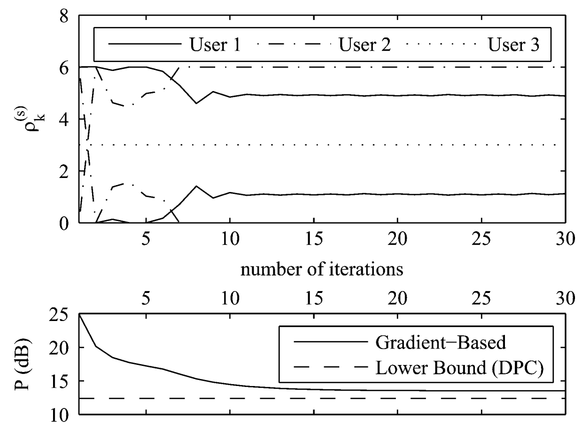

Fig. 5. Development of the per-stream rate targets and the sum transmit power in a three-user system with $\rho_0 = 3$ bits per channel use.

The last curve in the plot is the optimal solution when DPC and time-sharing is allowed. This solution can be computed by means of convex optimization methods as described in [7]–[9]. It is not clear which portion of the power gap between the gradient-based scheme and the DPC optimum is a result of the suboptimality of the gradient-based method and which portion is due to the restriction to linear transceivers without time-sharing. Nevertheless, it can be seen that the gap is relatively small, which means that the method proposed in this paper performs close to the globally optimal solution.

In Fig. 5, we can observe how the per-stream rate targets of the various streams behave from one iteration to the next for a typical channel realization in a system with $M = 4$ base station antennas, $K = 3$ users, $N_k = 2$ antennas at each user terminal k, and $\rho_0 = 3$ bits per channel use. Note that as requested, the sum of the per-stream rate targets $\sum_{s=1}^{S_k} \rho_k^{(s)}$ of user $k \in \{1, 2\}$ is $2\rho_0$ in each iteration while the sum of the per-stream rate targets of user $k = 3$ is always ρ_0. In this plot, we can observe that the algorithm can indeed activate inactive streams if this leads to a decreased sum transmit power. As can be seen, such an activation of an additional data stream can even lead to situations where the number of active streams exceeds the degrees of freedom M. However, in the simulation shown in Fig. 5, a stream is deactivated later during the execution of the algorithm so that after convergence, the number of active streams is not larger than M.

In Fig. 5, we can also observe that the sum transmit power is monotonically non-increasing from one iteration to the next and eventually converges. The resulting sum transmit power is again relatively close to the optimal DPC solution, which we have plotted as a lower bound. However, we can observe in Fig. 5 that the per-stream rate targets might oscillate. In fact, in Section VI, we have only shown convergence of the cost function, which does not necessarily imply convergence of the optimization variables. Based on the plot, we cannot tell whether or not the rate targets eventually converge for a higher number of iterations. However, from a practical point of view, there is no need to wait for converged rate targets since all strategies that appear in the oscillation have nearly the same sum transmit power, i.e., any of them can be used.

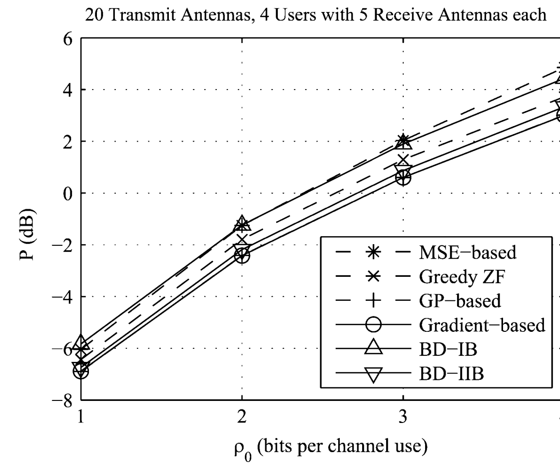

Fig. 6. Transmit power for different per-user rate requirements.

Note that Fig. 5 does not show the development of the per-stream rate targets within one iteration. Therefore, we have visualized the targets $\rho_1^{(1)}$ and $\rho_1^{(2)}$ of user 1 during iteration 5 through 7 in Fig. 3, which was discussed earlier in this paper.

In order to be able to compare the proposed algorithm to the method from [17], we have also performed simulations in a setting with $K = 4$ users and $N_k = 5$ receive antennas for all users k, where the number of transmit antennas is increased to $M = \sum_{k=1}^{K} N_k = 20$. In this scenario, the base station has a sufficiently high number of degrees of freedom to perform block-diagonalization [21]. The results can be seen in Fig. 6. The additional methods considered in this figure are block-diagonalization with interference balancing (BD-IB) and block-diagonalization with iterative interference balancing (BD-IIB). The block-diagonalization method with interference balancing [17] computes the per-stream rate targets and the downlink receive filters using the block-diagonalization scheme [21] while the downlink beamformers (including the power allocation) are found by an interference balancing method. This balancing is equivalent to the evaluation of the function $\mathcal{Q}$ defined in (20) and can thus be performed, e.g., using the method from [22]. In the block-diagonalization algorithm with iterative interference balancing [17], the downlink receive filters are optimized as well. This is done by iteratively performing updates of the transmit and receive filters in an alternating manner. While the authors of [17] did not observe a notable performance difference between the two schemes, a significant decrease in sum transmit power is achieved by the BD-IIB scheme in our simulation setup.

In fact, the BD-IIB scheme performs close to the solution of the gradient-based and the GP-based method. The reason is that the per-stream rate targets obtained from the block-diagonalization are a quite good choice in most cases, and the filter update procedure is similar as in the proposed algorithm (apart from the missing diagonalization of the MSE matrices). However, block-diagonalization can only be applied to systems where the number of transmit antennas is at least as high as the total number of receive antennas $(M \geq \sum_{k=1}^{K} N_k)$. This assumption, which is not necessarily fulfilled in practical systems, is not needed for the proposed gradient-based algorithm.

The performance of the BD-IB method without the additional iteration is similar to the solution found by the MSE-based

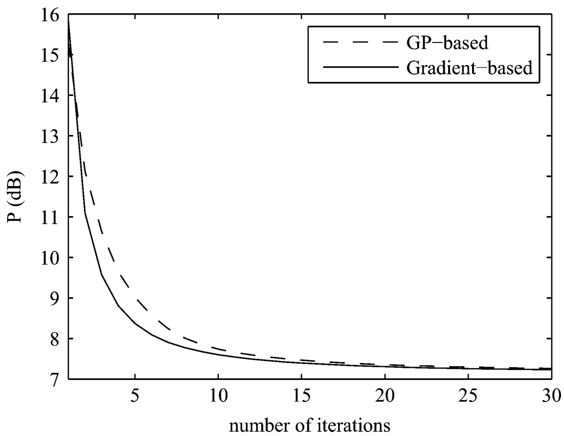

Fig. 7. Convergence of the GP-based and the gradient-based algorithm for $\rho_0 = 4$ bits per channel use.

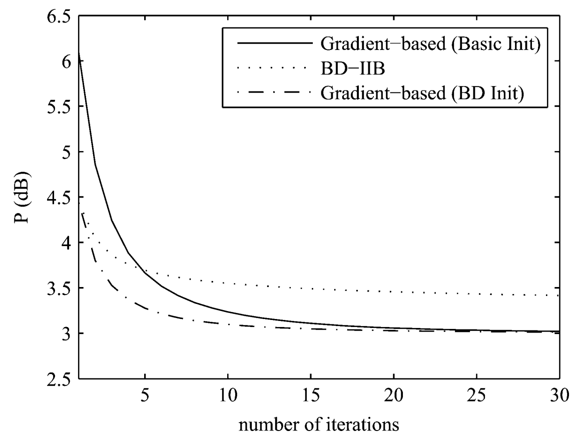

Fig. 8. Convergence of the BD-IIB scheme and the gradient-based algorithm with different initializations for $\rho_0 = 4$ bits per channel use.

power minimization from [20]. Also note that the latter has lost its disastrous behavior for high rate requirements due to the increased number of degrees of freedom in the system with $M = 20$ base station antennas.

VIII. Computational Complexity

Due to the complicatedness of the considered algorithms, a detailed quantitative complexity analysis would go beyond the scope of this paper. Instead, the aim of this section is to qualitatively discuss the speed of convergence of the various algorithms (measured by the number of iterations), and to investigate the complexity of the steps within one iteration.

The reduction of the transmit powers during the execution of the gradient-projection algorithm and the geometric programming based algorithm is plotted for the system with $M = 10$, $K = 4$, $N_k = 5\,\forall k$ in Fig. 7, averaged over 1000 channel realizations. It can be seen that the new gradient-based algorithm arrives at small values of the sum transmit power with less iterations than the GP-based method from [19].

In addition, the authors of [19] acknowledge that "power allocation with GP has high complexity." This fact might be surprising at the first glance since it is well known that geometric programs can be solved in reasonable time by converting them to equivalent convex programs. However, the problem of the GP-based method is that not only one geometric program has to be solved, but the solution to a geometric program in $\sum_{k=1}^{K} N_k$ variables has to be found in each iteration. Therefore, the complexity of solving a geometric program does not have to be compared with the overall complexity of the proposed algorithm, but with the complexity of the operations within one iteration. Indeed, these operations of the proposed algorithm can be executed in significantly less time. The computationally most complex subproblem of the gradient-based approach is the repeated evaluation of the function $\mathcal{Q}$ defined in (20). This function is evaluated up to $\log_2 \frac{d_{\text{init}}}{d_{\min}}$ times. Depending on the required accuracy, this can be about ten to twenty times, but in most iterations, this limit is not reached. The fixed point iteration from [20], which can be used to evaluate the function, converges in a very small number of iterations (typically five to ten), and the inversion of a matrix $\in \mathbb{C}^{M\times M}$ is the most complex operation in each iteration. In our numerical simulations, this needed significantly less execution time than the rather complex procedure of solving a geometric program. The same is true for the inversion of a matrix $\in \mathbb{C}^{S_{\text{tot}}\times S_{\text{tot}}}$ in the computation of the gradient in (23) and of a matrix of the same size in the uplink-to-downlink transformation in (36), which are both performed once per outer iteration.

Clearly, another computationally complex step in the gradient-projection algorithm is the update of the filters of currently inactive streams, which comprises the inversion of a matrix $\in \mathbb{C}^{M\times M}$ and a matrix $\in \mathbb{C}^{S_{\text{act}}\times S_{\text{act}}}$, where S_{act} is the number of active streams, and the repeated computation of GEVDs. However, firstly, as the GEVDs involve matrices with moderate dimensions of less than $S_k \times S_k$, this step is also much less complex than the solution of the geometric program, and secondly, the filter update for inactive streams can even be skipped if a further complexity reduction is desired. By instead leaving the filters of inactive streams as they were in the previous iteration, the resulting sum transmit power was increased on average by no more than 0.15 dB in our numerical simulations.

Consequently, the gradient-projection algorithm proposed in this paper achieves the same performance as the geometric programming based method from [19] with a much lower computational complexity. Clearly, the actual difference in computation time depends on the solver used for the geometric programs.

Fig. 8 refers to the system with $M = 20$, $K = 4$, $N_k = 5\,\forall k$. Here, it can be seen that the sum transmit power resulting from the gradient-projection algorithm rapidly falls below the solution of the BD-IIB algorithm, even though the basic initialization that was proposed for the gradient scheme in Section VI is much worse than the initialization from the block-diagonalization. Furthermore, it turns out that initializing also the gradient-based method using the block-diagonalization scheme does not lead to a decreased sum transmit power on average, i.e., the changed initialization does not lead to more preferable solutions. Nevertheless, it speeds up the convergence of the algorithm.

It can also be seen from the plot that the number of iterations needed by the BD-IIB algorithm to come close to the final value lies in the same order as for the gradient-based scheme. However, as the BD-IIB does not update the per-stream rate targets and refrains from diagonalizing the MSE matrices, it has a lower complexity than the gradient-based scheme in each iteration. This gain in computational efficiency comes at the cost of an increased sum transmit power and the restriction to systems with $M \geq \sum_{k=1}^{K} N_k$. Note that systems with $M < \sum_{k=1}^{K} N_k$ can be solved with the new gradient-based scheme, but not with the BD-based methods.

IX. Conclusion

The problem of power minimization in MIMO broadcast channels with linear transceivers, which was considered in this paper, is a non-convex optimization problem. For non-convex problems, optimization techniques based on gradient steps or on alternating optimization are not able to find the globally optimal solution in general as they risk to converge to a solution that is far from the global optimum. On the other hand, such algorithms are interesting from a practical point of view as they can be implemented with a reasonable computational complexity.

Therefore, we have proposed a new power minimization algorithm, which is based on gradient-projection steps for new auxiliary variables called per-stream rate targets, and on an alternating optimization of the filters in the downlink and in the dual uplink. Although such an approach is suboptimal in general, we could demonstrate in numerical simulations that the average sum transmit power achieved by the gradient-based algorithm lies close to the lower bound given by the DPC solution. This implies that it also lies close to the globally optimal solution for linear transceivers.

A good performance was also observed for the algorithm from [18] and [19] based on a geometric programming formulation and for the block-diagonalization method with iterative interference balancing from [17]. However, the former has a high computational complexity, and the latter is restricted to broadcast channels with at least as many base station antennas as the total number of receive antennas. Both drawbacks do not apply to the gradient-based method proposed in this paper.

Appendix A

Proof of Proposition 1: We prove the equivalent statement that $\boldsymbol{J}_R^{\mathrm{T}}$ is inverse-positive. Since $\boldsymbol{J}_R^{\mathrm{T}}$ is a Z-matrix, i.e., $[\boldsymbol{J}_R^{\mathrm{T}}]_{i,j} \leq 0$ for $i \neq j$ [40, Ch. 6], it suffices to show that there exists a positive diagonal matrix $\boldsymbol{D}$ such that $\boldsymbol{J}_R^{\mathrm{T}}\boldsymbol{D}$ is strictly diagonally dominant, i.e., $[\boldsymbol{J}_R^{\mathrm{T}}\boldsymbol{D}]_{i,i} > \sum_{j\neq i} |[\boldsymbol{J}_R^{\mathrm{T}}\boldsymbol{D}]_{i,j}| \ \forall i$. Having shown this, it can be concluded, that $\boldsymbol{J}_R^{\mathrm{T}}$ is a nonsingular M-matrix, and thus, it is inverse-positive [40, Ch. 6, Theorem 2.3].

The partial derivatives $\frac{\partial R_\kappa^{(\sigma)}}{\partial q_{k'}^{(s')}}$ can be computed from (15) by means of standard matrix calculus as

$$\frac{\partial R_\kappa^{(\sigma)}}{\partial q_\kappa^{(\sigma)}} = \frac{\tilde{\boldsymbol{h}}_\kappa^{(\sigma),\mathrm{H}} \boldsymbol{X}_\kappa^{(\sigma),-1} \tilde{\boldsymbol{h}}_\kappa^{(\sigma)}}{\ln 2 \cdot \left(1 + q_\kappa^{(\sigma)} \tilde{\boldsymbol{h}}_\kappa^{(\sigma),\mathrm{H}} \boldsymbol{X}_\kappa^{(\sigma),-1} \tilde{\boldsymbol{h}}_\kappa^{(\sigma)}\right)} \tag{42}$$

and

$$\frac{\partial R_\kappa^{(\sigma)}}{\partial q_{k'}^{(s')}} = \frac{-q_\kappa^{(\sigma)} \left| \tilde{\boldsymbol{h}}_\kappa^{(\sigma),\mathrm{H}} \boldsymbol{X}_\kappa^{(\sigma),-1} \tilde{\boldsymbol{h}}_{k'}^{(s')} \right|^2}{\ln 2 \cdot \left(1 + q_\kappa^{(\sigma)} \tilde{\boldsymbol{h}}_\kappa^{(\sigma),\mathrm{H}} \boldsymbol{X}_\kappa^{(\sigma),-1} \tilde{\boldsymbol{h}}_\kappa^{(\sigma)}\right)} \tag{43}$$

for $(k', s') \neq (\kappa, \sigma)$, where $\boldsymbol{X}_\kappa^{(\sigma)}$ is defined in (16). Using the matrix $\boldsymbol{X}$ defined in (27) and applying the matrix inversion lemma,[11] we get

$$\begin{aligned} \boldsymbol{X}_\kappa^{(\sigma),-1} &= \left(\boldsymbol{X} - q_\kappa^{(\sigma)} \tilde{\boldsymbol{h}}_\kappa^{(\sigma)} \tilde{\boldsymbol{h}}_\kappa^{(\sigma),\mathrm{H}}\right)^{-1} \\ &= \boldsymbol{X}^{-1} - \frac{q_\kappa^{(\sigma)}}{\alpha_\kappa^{(\sigma)} - 1} \boldsymbol{X}^{-1} \tilde{\boldsymbol{h}}_\kappa^{(\sigma)} \tilde{\boldsymbol{h}}_\kappa^{(\sigma),\mathrm{H}} \boldsymbol{X}^{-1} \end{aligned} \tag{44}$$

with

$$\begin{aligned} \alpha_\kappa^{(\sigma)} &= q_\kappa^{(\sigma)} \tilde{\boldsymbol{h}}_\kappa^{(\sigma),\mathrm{H}} \boldsymbol{X}^{-1} \tilde{\boldsymbol{h}}_\kappa^{(\sigma)} \\ &= q_\kappa^{(\sigma)} \tilde{\boldsymbol{h}}_\kappa^{(\sigma),\mathrm{H}} \left(\boldsymbol{X}_\kappa^{(\sigma)} + q_\kappa^{(\sigma)} \tilde{\boldsymbol{h}}_\kappa^{(\sigma)} \tilde{\boldsymbol{h}}_\kappa^{(\sigma),\mathrm{H}}\right)^{-1} \tilde{\boldsymbol{h}}_\kappa^{(\sigma)} < 1 \end{aligned} \tag{45}$$

where the inequality can be shown by applying the matrix inversion lemma in (45). From (44), we find

$$\tilde{\boldsymbol{h}}_\kappa^{(\sigma),\mathrm{H}} \boldsymbol{X}_\kappa^{(\sigma),-1} \tilde{\boldsymbol{h}}_\kappa^{(\sigma)} = \tilde{\boldsymbol{h}}_\kappa^{(\sigma),\mathrm{H}} \boldsymbol{X}^{-1} \tilde{\boldsymbol{h}}_\kappa^{(\sigma)} \frac{1}{1 - \alpha_\kappa^{(\sigma)}}, \tag{46}$$

and

$$\begin{aligned} &- q_\kappa^{(\sigma)} \left| \tilde{\boldsymbol{h}}_\kappa^{(\sigma),\mathrm{H}} \boldsymbol{X}_\kappa^{(\sigma),-1} \tilde{\boldsymbol{h}}_{k'}^{(s')} \right|^2 \\ &\quad = -q_\kappa^{(\sigma)} \left| \tilde{\boldsymbol{h}}_\kappa^{(\sigma),\mathrm{H}} \boldsymbol{X}^{-1} \tilde{\boldsymbol{h}}_{k'}^{(s')} \right|^2 \left(\frac{1}{1 - \alpha_\kappa^{(\sigma)}} \right)^2. \end{aligned} \tag{47}$$

Now consider the matrix $\boldsymbol{J}_R^{\mathrm{T}}\boldsymbol{D}$, where $\boldsymbol{D}$ is the positive diagonal matrix $\boldsymbol{D} = \ln 2 \cdot \mathrm{blkdiag}\{\boldsymbol{D}_1, \ldots, \boldsymbol{D}_K\}$, and $\boldsymbol{D}_\kappa$ is a diagonal matrix with

$$[\boldsymbol{D}_\kappa]_{\sigma,\sigma} = \left(1 + q_\kappa^{(\sigma)} \tilde{\boldsymbol{h}}_\kappa^{(\sigma),\mathrm{H}} \boldsymbol{X}_\kappa^{(\sigma),-1} \tilde{\boldsymbol{h}}_\kappa^{(\sigma)}\right) \left(1 - \alpha_\kappa^{(\sigma)}\right)^2. \tag{48}$$

As can be easily verified,

$$\begin{aligned} &\left[\boldsymbol{J}_R^{\mathrm{T}}\boldsymbol{D}\right]_{\sigma + \sum_{j=1}^{\kappa-1} S_j,\ \sigma + \sum_{j=1}^{\kappa-1} S_j} \\ &\quad = \tilde{\boldsymbol{h}}_\kappa^{(\sigma),\mathrm{H}} \boldsymbol{X}^{-1} \tilde{\boldsymbol{h}}_\kappa^{(\sigma)} \left(1 - \alpha_\kappa^{(\sigma)}\right) \end{aligned} \tag{49}$$

and

$$\left[\boldsymbol{J}_R^{\mathrm{T}}\boldsymbol{D}\right]_{s' + \sum_{j=1}^{k'-1} S_j,\ \sigma + \sum_{j=1}^{\kappa-1} S_j} = -q_\kappa^{(\sigma)} \left| \tilde{\boldsymbol{h}}_\kappa^{(\sigma),\mathrm{H}} \boldsymbol{X}^{-1} \tilde{\boldsymbol{h}}_{k'}^{(s')} \right|^2 \tag{50}$$

for $(k', s') \neq (\kappa, \sigma)$, and due to

$$\begin{aligned} &\sum_{\substack{\kappa=1 \\ (\kappa,\sigma)\neq(k',s')}}^{K} \sum_{\sigma=1}^{S_\kappa} \left| -q_\kappa^{(\sigma)} \left| \tilde{\boldsymbol{h}}_\kappa^{(\sigma),\mathrm{H}} \boldsymbol{X}^{-1} \tilde{\boldsymbol{h}}_{k'}^{(s')} \right|^2 \right| \\ &= \sum_{\substack{\kappa=1 \\ (\kappa,\sigma)\neq(k',s')}}^{K} \sum_{\sigma=1}^{S_\kappa} \tilde{\boldsymbol{h}}_{k'}^{(s'),\mathrm{H}} \boldsymbol{X}^{-1} \tilde{\boldsymbol{h}}_\kappa^{(\sigma)} q_\kappa^{(\sigma)} \tilde{\boldsymbol{h}}_\kappa^{(\sigma),\mathrm{H}} \boldsymbol{X}^{-1} \tilde{\boldsymbol{h}}_{k'}^{(s')} \\ &= \tilde{\boldsymbol{h}}_{k'}^{(s'),\mathrm{H}} \boldsymbol{X}^{-1} \left(\boldsymbol{X} - \mathbf{I}_{S_{\mathrm{tot}}} - \tilde{\boldsymbol{h}}_{k'}^{(s')} q_{k'}^{(s')} \tilde{\boldsymbol{h}}_{k'}^{(s'),\mathrm{H}} \right) \boldsymbol{X}^{-1} \tilde{\boldsymbol{h}}_{k'}^{(s')} \\ &< \tilde{\boldsymbol{h}}_{k'}^{(s'),\mathrm{H}} \boldsymbol{X}^{-1} \left(\boldsymbol{X} - \tilde{\boldsymbol{h}}_{k'}^{(s')} q_{k'}^{(s')} \tilde{\boldsymbol{h}}_{k'}^{(s'),\mathrm{H}} \right) \boldsymbol{X}^{-1} \tilde{\boldsymbol{h}}_{k'}^{(s')} \\ &= \tilde{\boldsymbol{h}}_{k'}^{(s'),\mathrm{H}} \boldsymbol{X}^{-1} \tilde{\boldsymbol{h}}_{k'}^{(s')} \left(1 - \alpha_{k'}^{(s')}\right), \end{aligned} \tag{51}$$

$\boldsymbol{J}_R^{\mathrm{T}}\boldsymbol{D}$ is strictly diagonally dominant. ■

[11] $(\boldsymbol{A} + \boldsymbol{BCD})^{-1} = \boldsymbol{A}^{-1} - \boldsymbol{A}^{-1}\boldsymbol{B}(\boldsymbol{C}^{-1} + \boldsymbol{D}\boldsymbol{A}^{-1}\boldsymbol{B})^{-1}\boldsymbol{D}\boldsymbol{A}^{-1}$ (e.g., [41]).

APPENDIX B

Proof of Theorem 1: The partial derivatives can be written as

$$\frac{\partial P}{\partial \rho_k^{(s)}} = \frac{\partial \left(\sum_{k'=1}^{K} \sum_{s'=1}^{S_{k'}} q_{k'}^{(s')} \right)}{\partial \rho_k^{(s)}} = \sum_{k'=1}^{K} \sum_{s'=1}^{S_{k'}} \frac{q_{k'}^{(s')}}{\partial \rho_k^{(s)}}, \tag{52}$$

with

$$(\boldsymbol{q}_k)_{\forall k} = \mathcal{Q}\left(\left(\tilde{\boldsymbol{h}}_k^{(1)}, \ldots, \tilde{\boldsymbol{h}}_k^{(S_k)}, \boldsymbol{\rho}_k \right)_{\forall k} \right) \tag{53}$$

where $\mathcal{Q}$ is defined in (20). Using the chain rule and the fact that all rate constraints are fulfilled with equality in the solution of (18) [42], i.e., $R_k^{(s)} = \rho_k^{(s)}$, we have that

$$\sum_{k'=1}^{K} \sum_{s'=1}^{S_{k'}} \frac{\partial R_\kappa^{(\sigma)}}{\partial q_{k'}^{(s')}} \frac{\partial q_{k'}^{(s')}}{\partial \rho_k^{(s)}} = \frac{\partial R_\kappa^{(\sigma)}}{\partial \rho_k^{(s)}} = \delta_{k,\kappa} \delta_{s,\sigma} \tag{54}$$

for all k, s, κ, σ. Since the derivatives $\frac{\partial R_\kappa^{(\sigma)}}{\partial q_{k'}^{(s')}}$ are known [see (42) and (43)], we have S_{tot}^2 equations of the form (54) with the same number of unknowns $\frac{\partial q_{k'}^{(s')}}{\partial \rho_k^{(s)}}$. In matrix notation, this can be written as

$$\boldsymbol{J}_R \boldsymbol{J}_q = \mathbf{I}_{S_{\text{tot}}} \tag{55}$$

where $\boldsymbol{J}_q$ is the Jacobian matrix of the powers $q_{k'}^{(s')}$ with respect to the rate targets $\rho_k^{(s)}$, i.e.,

$$[\boldsymbol{J}_q]_{s'+\sum_{j=1}^{k'-1} S_j,\, s+\sum_{j=1}^{k-1} S_j} = \frac{\partial q_{k'}^{(s')}}{\partial \rho_k^{(s)}}. \tag{56}$$

Due to Proposition 1, a solution $\boldsymbol{J}_q = \boldsymbol{J}_R^{-1}$ exists, and this solution has non-negative entries. The desired partial derivatives $\frac{\partial P}{\partial \rho_k^{(s)}}$ are given by the column sums of $\boldsymbol{J}_R^{-1}$, which are non-negative. ∎

APPENDIX C

Proof of Lemma 1: To perform the projection to the set of per-stream rate targets feasible for user k, we have to minimize the Euclidean distance, i.e., the convex optimization problem

$$\min_{\boldsymbol{\rho}_k} \sum_{s=1}^{S_k} \left(\rho_k^{(s)} - \tilde{\rho}_k^{(s)} \right)^2$$
$$\text{s.t. } \boldsymbol{\rho}_k \geq \mathbf{0} \text{ and } \sum_{s=1}^{S_k} \rho_k^{(s)} = \varrho_k \tag{57}$$

has to be solved (cf., e.g., [43] and [44]). Introducing Lagrangian multipliers $\lambda_k^{(s)}\ \forall s \in \{1, \ldots, S_k\}$ and μ_k', the KKT conditions (cf., e.g., [44]) of this problem read as

$$0 = 2(\rho_k^{(s)} - \tilde{\rho}_k^{(s)}) - \lambda_k^{(s)} - \mu_k'\ \forall s \tag{58}$$
$$\rho_k^{(s)} \geq 0\ \forall s \text{ and } \lambda_k^{(s)} \geq 0\ \forall s \text{ and } \lambda_k^{(s)} \rho_k^{(s)} = 0\ \forall s \tag{59}$$
$$\sum_{s=1}^{S_k} \rho_k^{(s)} = \varrho_k \text{ and } \mu_k' \in \mathbb{R}. \tag{60}$$

From (58) and (59), we get the waterfilling equation

$$\rho_k^{(s)} = \max\left\{ \tilde{\rho}_k^{(s)} + \mu_k,\ 0 \right\} \tag{61}$$

where the optimal water level $\mu_k = \frac{\mu_k'}{2} \in \mathbb{R}$ can be obtained from (60) as

$$\varrho_k = \sum_{s \in \mathcal{S}_{k,\text{a}}} \left(\tilde{\rho}_k^{(s)} + \mu_k \right)$$
$$\Leftrightarrow \mu_k = \frac{1}{|\mathcal{S}_{k,\text{a}}|} \left(\varrho_k - \sum_{s \in \mathcal{S}_{k,\text{a}}} \tilde{\rho}_k^{(s)} \right) \tag{62}$$

with $\mathcal{S}_{k,\text{a}}$ being the set of active streams of user k. ∎

APPENDIX D
FILTER UPDATE FOR INACTIVE STREAMS

In this Appendix, we propose an update method for the filters belonging to currently inactive streams, i.e., streams with $p_k^{(s)} = q_k^{(s)} = 0$. Non-zero equalizers $\boldsymbol{v}_k^{(s),\text{H}}$ are necessary for these streams in order to provide effective MISO channels $\tilde{\boldsymbol{h}}_k^{(s),\text{H}}$. The aim of the update is to create streams that are likely to be activated in the next rate target update and do not interfere with other streams of the same user.

The demand of zero interference, i.e., $\boldsymbol{v}_k^{(s),\text{H}} \boldsymbol{H}_k^{\text{H}} \check{\boldsymbol{b}}_k^{(s')} = 0$ for $s' \neq s$ and for all s that correspond to inactive streams obviously makes sense: this condition is the counterpart of the requirement of a diagonal MSE matrix, which we imposed for the active streams. Note that the condition is automatically fulfilled for all s' that correspond to currently inactive streams with $p_k^{(s')} = 0$ since $\check{\boldsymbol{b}}_k^{(s')} = p_k^{(s')} \boldsymbol{b}_k^{(s')} = \mathbf{0}$ in this case. Let $\boldsymbol{\Phi}_k$ denote a matrix of basis vectors of the null space of $\check{\boldsymbol{B}}_k^{\text{H}} \boldsymbol{H}_k$. Then, any downlink receive filter fulfilling the condition of zero interference can be expressed as $\boldsymbol{v}_k^{(s)} = \boldsymbol{\Phi}_k \hat{\boldsymbol{v}}_k^{(s)}$, where $\hat{\boldsymbol{v}}_k^{(s)}$ is a vector of appropriate size without special structure.

We want that there is at least one stream that has good chances to get active during the next update of the rate targets, which is the case if the derivative $\frac{\partial P}{\partial \rho_k^{(s)}}$ is small. Let us reorder the columns and rows of the Jacobian matrix $\boldsymbol{J}_R$ defined in (22) such that the reordered version $\tilde{\boldsymbol{J}}_R$ can be partitioned into

$$\tilde{\boldsymbol{J}}_R = \begin{bmatrix} \boldsymbol{J}_{R,\text{aa}} & \boldsymbol{J}_{R,\text{ai}} \\ \boldsymbol{J}_{R,\text{ia}} & \boldsymbol{J}_{R,\text{ii}} \end{bmatrix} \tag{63}$$

where the first letter in the second subscript refers to rows belonging to active (a) or inactive (i) streams, and the second letter refers to the columns. For instance, $\boldsymbol{J}_{R,\text{ia}}$ contains the derivatives $\frac{\partial R_\kappa^{(\sigma)}}{\partial q_{k'}^{(s')}}$ with ${}_\kappa^{(\sigma)}$ corresponding to inactive and ${}_{k'}^{(s')}$ corresponding to active streams. As can be easily verified, $\frac{\partial R_\kappa^{(\sigma)}}{\partial q_{k'}^{(s')}} = 0$ if ${}_\kappa^{(\sigma)}$ is inactive and ${}_\kappa^{(\sigma)} \neq {}_{k'}^{(s')}$. Thus, [45]

$$\tilde{\boldsymbol{J}}_R^{-1} = \begin{bmatrix} \boldsymbol{J}_{R,\text{aa}} & \boldsymbol{J}_{R,\text{ai}} \\ \mathbf{0} & \boldsymbol{J}_{R,\text{ii}} \end{bmatrix}^{-1} = \begin{bmatrix} \boldsymbol{J}_{R,\text{aa}}^{-1} & -\boldsymbol{J}_{R,\text{aa}}^{-1} \boldsymbol{J}_{R,\text{ai}} \boldsymbol{J}_{R,\text{ii}}^{-1} \\ \mathbf{0} & \boldsymbol{J}_{R,\text{ii}}^{-1} \end{bmatrix} \tag{64}$$

with the diagonal matrix

$$\boldsymbol{J}_{R,\text{ii}} = \frac{1}{\ln 2} \text{diag}\left\{ \tilde{\boldsymbol{h}}_\kappa^{(\sigma),\text{H}} \boldsymbol{X}_\kappa^{(\sigma),-1} \tilde{\boldsymbol{h}}_\kappa^{(\sigma)} \right\}. \tag{65}$$

Applying Theorem 1 and using $\tilde{\boldsymbol{e}}_\kappa^{(\sigma)}$ to denote the accordingly reordered version of $\boldsymbol{e}_\kappa^{(\sigma)}$, we get for an inactive stream $_\kappa^{(\sigma)}$:

$$\begin{aligned}\frac{\partial P}{\partial \rho_\kappa^{(\sigma)}} &= \mathbf{1}^{\mathrm{T}} \boldsymbol{J}_R^{-1} \boldsymbol{e}_\kappa^{(\sigma)} = \mathbf{1}^{\mathrm{T}} \tilde{\boldsymbol{J}}_R^{-1} \tilde{\boldsymbol{e}}_\kappa^{(\sigma)} \\ &= \frac{\ln 2}{\tilde{\boldsymbol{h}}_\kappa^{(\sigma),\mathrm{H}} \boldsymbol{X}_\kappa^{(\sigma),-1} \tilde{\boldsymbol{h}}_\kappa^{(\sigma)}} \mathbf{1}^{\mathrm{T}} \begin{bmatrix} -\boldsymbol{J}_{R,\mathrm{aa}}^{-1} \boldsymbol{J}_{R,\mathrm{ai}} \boldsymbol{e}_{\mathrm{i},\kappa}^{(\sigma)} \\ \boldsymbol{e}_{\mathrm{i},\kappa}^{(\sigma)} \end{bmatrix} \\ &= \ln 2 \cdot \frac{\boldsymbol{v}_\kappa^{(\sigma),\mathrm{H}} \left(\mathbf{I}_{N_\kappa} + \boldsymbol{H}_\kappa^{\mathrm{H}} \boldsymbol{A} \boldsymbol{H}_\kappa \right) \boldsymbol{v}_\kappa^{(\sigma)}}{\boldsymbol{v}_\kappa^{(\sigma),\mathrm{H}} \boldsymbol{H}_\kappa^{\mathrm{H}} \boldsymbol{X}^{-1} \boldsymbol{H}_\kappa \boldsymbol{v}_\kappa^{(\sigma)}} \end{aligned} \tag{66}$$

where $\boldsymbol{e}_{\mathrm{i},\kappa}^{(\sigma)}$ is the canonical unit vector that identifies the stream $_\kappa^{(\sigma)}$ among all inactive streams, and $\boldsymbol{A}$ is given by

$$\boldsymbol{A} = \sum_{_k^{(s)}:\ \mathrm{active}} \frac{\mathbf{1}^{\mathrm{T}} \boldsymbol{J}_{R,\mathrm{aa}}^{-1} \boldsymbol{e}_{\mathrm{a},k}^{(s)} \cdot \boldsymbol{X}_k^{(s),-1} \tilde{\boldsymbol{h}}_k^{(s)} q_k^{(s)} \tilde{\boldsymbol{h}}_k^{(s),\mathrm{H}} \boldsymbol{X}_k^{(s),-1}}{\ln 2 \cdot \left(1 + q_k^{(s)} \tilde{\boldsymbol{h}}_k^{(s),\mathrm{H}} \boldsymbol{X}_k^{(s),-1} \tilde{\boldsymbol{h}}_k^{(s)} \right)} \tag{67}$$

where $\boldsymbol{e}_{\mathrm{a},k}^{(s)}$ is the canonical unit vector that identifies the stream $_k^{(s)}$ among all active streams.

Thus, in order to find a good filter for the first considered inactive stream of a user, we have to solve the optimization problem

$$\boldsymbol{v}_\kappa^{(\sigma)} = \boldsymbol{\Phi}_\kappa \operatorname*{argmin}_{\hat{\boldsymbol{v}}_\kappa^{(\sigma)}} \frac{\hat{\boldsymbol{v}}_\kappa^{(\sigma),\mathrm{H}} \boldsymbol{\Phi}_\kappa^{\mathrm{H}} \left(\mathbf{I}_{N_\kappa} + \boldsymbol{H}_\kappa^{\mathrm{H}} \boldsymbol{A} \boldsymbol{H}_\kappa \right) \boldsymbol{\Phi}_\kappa \hat{\boldsymbol{v}}_\kappa^{(\sigma)}}{\hat{\boldsymbol{v}}_\kappa^{(\sigma),\mathrm{H}} \boldsymbol{\Phi}_\kappa^{\mathrm{H}} \boldsymbol{H}_\kappa^{\mathrm{H}} \boldsymbol{X}^{-1} \boldsymbol{H}_\kappa \boldsymbol{\Phi}_\kappa \hat{\boldsymbol{v}}_\kappa^{(\sigma)}} \tag{68}$$

which is a generalized eigenvalue problem, i.e., the optimal $\hat{\boldsymbol{v}}_\kappa^{(\sigma)}$ is the generalized eigenvector of the matrices $\boldsymbol{\Phi}_\kappa^{\mathrm{H}} \left(\mathbf{I}_{N_\kappa} + \boldsymbol{H}_\kappa^{\mathrm{H}} \boldsymbol{A} \boldsymbol{H}_\kappa \right) \boldsymbol{\Phi}_\kappa \in \mathbb{C}^{S_{0,k} \times S_{0,k}}$ and $\boldsymbol{\Phi}_\kappa^{\mathrm{H}} \boldsymbol{H}_\kappa^{\mathrm{H}} \boldsymbol{X}^{-1} \boldsymbol{H}_\kappa \boldsymbol{\Phi}_\kappa \in \mathbb{C}^{S_{0,k} \times S_{0,k}}$ that belongs to the smallest generalized eigenvalue. Here, $S_{0,k} < S_k$ denotes the dimensionality of the null space of $\check{\boldsymbol{B}}_k^{\mathrm{H}} \boldsymbol{H}_k$. Without loss of generality, we can scale $\boldsymbol{v}_\kappa^{(\sigma)}$ to unit norm. Having found the filter $\boldsymbol{v}_\kappa^{(\sigma)}$ for an inactive stream, we replace $\boldsymbol{\Phi}_\kappa$ with a matrix of basis vectors of the null space of $[\check{\boldsymbol{B}}_k^{\mathrm{H}} \boldsymbol{H}_k,\ \boldsymbol{v}_\kappa^{(\sigma)}]^{\mathrm{H}}$ to ensure that a different direction is chosen for the next considered inactive stream of a user, and so on.

References

[1] M. Kobayashi and G. Caire, "A practical approach for weighted rate sum maximization in MIMO-OFDM broadcast channels," in *Conf. Rec. Asilomar*, Nov. 2007, pp. 1591–1595.

[2] M. Codreanu, A. Tölli, M. Juntti, and M. Latva-aho, "Joint design of Tx-Rx beamformers in MIMO downlink channel," *IEEE Trans. Signal Process.*, vol. 55, no. 9, pp. 4639–4655, Sep. 2007.

[3] S. Shi, M. Schubert, and H. Boche, "Weighted sum-rate optimization for multiuser MIMO systems," in *Proc. Conf. Inf. Sci. and Syst. (CISS)*, Mar. 2007, pp. 425–430.

[4] T. Yoo and A. Goldsmith, "On the optimality of multiantenna broadcast scheduling using zero-forcing beamforming," *IEEE J. Sel. Areas Commun.*, vol. 24, no. 3, pp. 528–541, Mar. 2006.

[5] A. D. Dabbagh and D. J. Love, "Precoding for multiple antenna Gaussian broadcast channels with successive zero-forcing," *IEEE Trans. Signal Process.*, vol. 55, no. 7, pp. 3837–3850, Jul. 2007.

[6] C. Guthy, W. Utschick, R. Hunger, and M. Joham, "Efficient weighted sum rate maximization with linear precoding," *IEEE Trans. Signal Process.*, vol. 58, no. 4, pp. 2284–2297, Apr. 2010.

[7] J. Lee and N. Jindal, "Symmetric capacity of MIMO downlink channels," in *Proc. Int. Symp. Inf. Theory (ISIT)*, Jul. 2006, pp. 1031–1035.

[8] G. Wunder and T. Michel, "Minimum rates scheduling for MIMO OFDM broadcast channels," in *Proc. Int. Symp. Spread Spectrum Tech. Appl. (ISSSTA)*, Aug. 2006, pp. 510–514.

[9] M. Mohseni, R. Zhang, and J. Cioffi, "Optimized transmission for fading multiple-access and broadcast channels with multiple antennas," *IEEE J. Sel. Areas Commun.*, vol. 24, no. 8, pp. 1627–1639, Aug. 2006.

[10] C.-H. F. Fung, W. Yu, and T. J. Lim, "Multi-antenna downlink precoding with individual rate constraints: Power minimization and user ordering," in *Proc. 9th Int. Conf. Commun. Syst. (ICCS) 2004*, Sep. 2004, pp. 45–49.

[11] W. W. L. Ho and Y.-C. Liang, "Efficient power minimization for MIMO broadcast channels with BD-GMD," in *Proc. Int. Conf. Commun. (ICC)*, Jun. 2007, pp. 2791–2796.

[12] W. W. L. Ho and Y.-C. Liang, "User ordering and subchannel selection for power minimization in MIMO broadcast channels using BD-GMD," in *Proc. Veh. Technol. Conf. (VTC) 2008-Fall*, Calgary, AB, Canada, Sep. 21–24, 2008, pp. 1–5.

[13] C. Guthy, W. Utschick, and G. Dietl, "Spatial resource allocation for the multiuser multicarrier MIMO broadcast channel—A QoS optimization perspective," in *Proc. Int. Conf. Acoust., Speech, Signal Process. (ICASSP)*, Mar. 2010, pp. 3166–3169.

[14] U. Erez and S. t. Brink, "A close-to-Capacity dirty paper coding scheme," *IEEE Trans. Inf. Theory*, vol. 51, no. 10, pp. 3417–3432, Oct. 2005.

[15] N. Hassan and M. Assaad, "Margin adaptive resource allocation in downlink multiuser MIMO-OFDMA system with multiuser eigenmode transmission," in *Proc. Int. Workshop Signal Process. Adv. Wireless Commun. (SPAWC)*, Jul. 2008, pp. 545–549.

[16] N. Hassan and M. Assaad, "Low complexity margin adaptive resource allocation in downlink MIMO-OFDMA system," *IEEE Trans. Wireless Commun.*, vol. 8, no. 7, pp. 3365–3371, Jul. 2009.

[17] Q. H. Spencer, A. L. Swindlehurst, and M. Haardt, "Fast power minimization with QoS constraints in multi-user MIMO downlinks," in *Proc. Int. Conf. Acoust., Speech, Signal Process. (ICASSP)*, Apr. 2003, vol. 4, pp. IV-816–IV-819.

[18] S. Shi, M. Schubert, and H. Boche, "Capacity balancing for multiuser MIMO systems," in *Proc. Int. Conf. Acoust., Speech, Signal Process. (ICASSP)*, Apr. 2007, vol. 3, pp. III-397–III-400.

[19] S. Shi, M. Schubert, and H. Boche, "Rate optimization for multiuser MIMO systems with linear processing," *IEEE Trans. Signal Process.*, vol. 56, no. 8, pp. 4020–4030, Aug. 2008.

[20] A. Mezghani, M. Joham, R. Hunger, and W. Utschick, "Transceiver design for multi-user MIMO systems," presented at the Int. ITG Workshop on Smart Antennas (ITG WSA), Ulm, Germany, Mar. 13–14, 2006.

[21] Q. H. Spencer, A. L. Swindlehurst, and M. Haardt, "Zero-forcing methods for downlink spatial multiplexing in multiuser MIMO channels," *IEEE Trans. Signal Process.*, vol. 52, no. 2, pp. 461–471, Feb. 2004.

[22] M. Schubert and H. Boche, "Solution of the multiuser downlink beamforming problem with individual SINR constraints," *IEEE Trans. Veh. Technol.*, vol. 53, no. 1, pp. 18–28, Jan. 2004.

[23] A. Khachan, A. Tenenbaum, and R. Adve, "Linear processing for the downlink in multiuser MIMO systems with multiple data streams," in *Proc. Int. Conf. Commun. (ICC)*, Jun. 2006, vol. 9, pp. 4113–4118.

[24] M. Schubert, S. Shi, and H. Boche, "Iterative transceiver optimization for linear multiuser MIMO channels with per-user MMSE requirements," presented at the EUSIPCO, Florence, Italy, Sep. 4–8, 2006.

[25] E. Jorswieck and H. Boche, "Rate balancing for the multi-antenna Gaussian broadcast channel," *Proc. Int. Symp. Spread Spectrum Tech. Appl. (ISSSTA)*, vol. 2, pp. 545–549, Sep. 2002.

[26] P. Tejera, W. Utschick, J. Nossek, and G. Bauch, "Rate balancing in multiuser MIMO OFDM systems," *IEEE Trans. Commun.*, vol. 57, no. 5, pp. 1370–1380, May 2009.

[27] C. Hellings, M. Joham, and W. Utschick, "Gradient-based rate balancing for MIMO broadcast channels with linear precoding," presented at the Int. ITG Workshop on Smart Antennas (ITG WSA), Aachen, Germany, Feb. 24–25, 2011.

[28] T. Michel and G. Wunder, "Achieving QoS and efficiency in the MIMO downlink with limited power," presented at the Int. ITG Workshop on Smart Antennas (ITG WSA), Vienna, Austria, Feb. 26–27, 2007.

[29] C. Guthy, W. Utschick, G. Bauch, and J. A. Nossek, "Sum throughput enhancements in quality of service constrained multiuser MIMO systems," *Wireless Pers. Commun.*, vol. 48, no. 1, pp. 157–173, 2009.

[30] J. G. Klotz, F. Knabe, and C. Huppert, "Resource allocation algorithms for minimum rates scheduling in MIMO-OFDM systems," in *Multi-Carrier Systems & Solutions*, ser. Lecture Notes in Electrical Engineering, S. Plass, A. Dammann, S. Kaiser, and K. Fazel, Eds. Dordrecht, The Netherlands: Springer, 2009, vol. 41, pp. 79–88.

[31] C. Huppert, F. Knabe, and J. Klotz, "User assignment for minimum rate requirements in OFDM-MIMO broadcast systems," *Electron. Lett.*, vol. 45, no. 12, pp. 621–623, Apr. 2009.

[32] G. Zheng, K.-K. Wong, and T.-S. Ng, "Throughput maximization in linear multiuser MIMO-OFDM downlink systems," *IEEE Trans. Veh. Technol.*, vol. 57, no. 3, pp. 1993–1998, May 2008.

[33] M. Chiang, C. W. Tan, D. Palomar, D. O'Neill, and D. Julian, "Power control by geometric programming," *IEEE Trans. Wireless Commun.*, vol. 6, no. 7, pp. 2640–2651, Jul. 2007.

[34] M. Joham and R. Hunger, "Feasible rate region of the MIMO broadcast channel with linear transceivers," in *Proc. Int. ITG Workshop Smart Antennas (ITG WSA)*, Feb. 2010, pp. 342–349.

[35] R. Hunger and M. Joham, "A general rate duality of the MIMO multiple access channel and the MIMO broadcast channel," presented at the IEEE GLOBECOM, New Orleans, LA, Nov. 30–Dec. 4, 2008.

[36] R. Hunger and M. Joham, "A complete description of the QoS feasibility region in the vector broadcast channel," *IEEE Trans. Signal Process.*, vol. 58, no. 7, pp. 3870–3878, Jul. 2010.

[37] P. Viswanath and D. N. C. Tse, "Sum capacity of the vector Gaussian broadcast channel and uplink-downlink duality," *IEEE Trans. Inf. Theory*, vol. 49, no. 8, pp. 1912–1921, Aug. 2003.

[38] G. Scutari, D. P. Palomar, and S. Barbarossa, "Optimal linear precoding strategies for wideband noncooperative systems based on game theory—Part II: Algorithms," *IEEE Trans. Signal Process.*, vol. 56, no. 3, pp. 1250–1267, Mar. 2008.

[39] P. Stoica, Y. Jiang, and J. Li, "On MIMO channel capacity: An intuitive discussion," *IEEE Signal Process. Mag.*, vol. 22, no. 3, pp. 83–84, May 2005.

[40] A. Berman and R. J. Plemmons, *Nonnegative Matrices in the Mathematical Sciences*, ser. Classics in Applied Mathematics. Philadelphia, PA: SIAM, 1994, vol. 9.

[41] R. A. Horn and C. R. Johnson, *Matrix Analysis*. Cambridge, U.K.: Cambridge Univ. Press, 1985.

[42] E. Visotsky and U. Madhow, "Optimum beamforming using transmit antenna arrays," in *Proc. Veh. Technol. Conf. (VTC)*, Jul. 1999, vol. 1, pp. 851–856.

[43] G. P. McCormick and R. A. Tapia, "The gradient projection method under mild differentiability conditions," *SIAM J. Control Optim.*, vol. 10, no. 1, pp. 93–98, Feb. 1972.

[44] M. S. Bazaraa, H. D. Sherali, and C. M. Shetty, *Nonlinear Programming: Theory and Algorithms*, 3rd ed. New York: Wiley-Interscience, 2006.

[45] F. Zhang, *The Schur complement and its applications*. New York: Springer Science+Business Media, 2005.

Christoph Hellings (S'10) received the B.Sc. degree and the Diploma degree in electrical engineering (both with Hons.) from the Technische Universität München (TUM) in 2008 and 2010, respectively.

He is currently working towards the Ph.D. degree at the Associate Institute for Signal Processing, TUM. His research interests include energy efficient communications and the optimization of linear precoding strategies in multi-carrier systems.

Mr. Hellings was awarded a scholarship of the Max Weber Program of the Bavarian state, and for his Diploma thesis, he received an award of the German Association for Electrical, Electronic & Information Technologies (VDE).

Michael Joham (M'04) was born in Kufstein, Austria, in 1974. He received the Dipl.-Ing. and Dr.-Ing. degrees (both *summa cum laude*) in electrical engineering from the Technische Universität München (TUM), Germany, in 1999 and 2004, respectively.

He was with the Institute for Circuit Theory and Signal Processing at the TUM from 1999 to 2004. Since 2004, he has been with the Associate Institute for Signal Processing at the TUM, where he is currently a Senior Researcher. In summers 1998 and 2000, he visited Purdue University, West Lafayette, IN. In spring 2007, he was a Guest Lecturer at the University of A Coruna, Spain. In spring 2008, he was a Guest Lecturer at the University of the German Federal Armed Forces, Munich, Germany, and a Guest Professor at the University of A Coruna, Spain. In winter 2009, he was a Guest Lecturer at the University of Hanover, Germany. In fall 2010 and 2011, he was a Guest Lecturer at the Singapore Institute of Technology. His current research interests are precoding in mobile and satellite communications, limited rate feedback, MIMO communications, and robust signal processing.

Dr. Joham received the VDE Preis for his Diploma thesis in 1999 and the Texas-Instruments-Preis for his dissertation in 2004. In 2007, he was a corecipient of the Best Paper Award at the International ITG/IEEE Workshop on Smart Antennas in Vienna.

Wolfgang Utschick (SM'06) was born on May 6, 1964. He completed several industrial education programs before he received the Diploma and Ph.D. degrees (both with Hons.), in electrical engineering, from the Technische Universität München, Germany (TUM), in 1993 and 1998, respectively.

During this period, he held a scholarship of the Bavarian Ministry of Education for exceptional students. From 1998 to 2002, he codirected the Signal Processing Group of the Institute of Circuit Theory and Signal Processing, TUM. Since 2000, he has been consulting in 3 GPP standardization in the field of multielement antenna systems. In 2002, he was appointed Professor at the TUM, where he is currently Head of the Fachgebiet Methoden der Signalverarbeitung. He teaches courses on signal processing, stochastic processes, and optimization theory in the field of digital communications. He is an Editor and Founder of the Springer Book Series *Foundations in Signal Processing, Communications and Networking*.

Dr. Utschick was awarded in 2006 for his excellent teaching records at TUM, and in 2007 received the ITG Award of the German Society for Information Technology (ITG). He is a senior member of the German VDE/ITG, where he has been appointed to the Expert Committee for Information and System Theory in 2009. He is currently also serving as a Chairman of the national DFG Focus Program Communications in Interference Limited Networks (COIN). He is an Associate Editor for the IEEE TRANSACTIONS ON SIGNAL PROCESSING. Since 2010, he has served for the IEEE Signal Processing Society as an elected member of the Technical Committee of Signal Processing for Communications and Networking.